The QuantiSlakeTest, measuring soil structural stability by dynamic underwater weighing

Frédéric M. Vanwindekens[1, *] and Brieuc F. Hardy[1, *]

[1]Department of Sustainability, Systems & Prospective – Unit of Soil, Water and Integrated Crop Production, Walloon Agricultural Research Centre, Rue du Bordia, 4, B-5030 Gembloux, Belgium
[*]These authors contributed equally to this work.

Correspondence: Frédéric M. Vanwindekens (f.vanwindekens@cra.wallonie.be) and Brieuc F. Hardy (b.hardy@cra.wallonie.be)

Abstract. We evaluated the performance of a new, simple test to evaluate soil structural stability. The QuantiSlakeTest (QST) consists in a quantitative approach of the slake test, a dynamic weighing of a dried structured soil sample once immersed in water. The objective of this work was threefold: we aimed to (i) derive indicators from QST curves to evaluate soil structural stability; (ii) establish the relationship between soil properties and QST indicators; and (iii) assess how QST indicators respond to contrasting soil management practices. To meet these goals, we sampled the soil of 35 plots from three long-term field trials in the silt loam region of Belgium dealing respectively with contrasting organic matter inputs, tillage and P-K fertilisation. For each plot, indicators calculated from QST curves (e. g. total relative mass loss, disaggregation speed, time to meet a threshold values of mass loss, ...) were compared to the results of the three tests of Le Bissonnais (1996), used as a reference method for the measurement of soil aggregate stability.

Shortly after immersion in water, soil mass increases due to the rapid replacement of air by water in soil porosity. Then soil mass reaches a maximum before decreasing, once mass loss by disaggregation exceeds mass gain by air loss. Our results confirmed that the early mass loss under water is mainly related to slaking, whereas after a longer time period, clay dispersion and differential swelling become the dominant processes of soil disaggregation. The overall soil structural stability was positively correlated to the soil organic carbon (SOC) content and negatively correlated to the clay content of soil. ~~Accordingly~~, consequently the SOC:clay ratio was closely related to QST indicators. Nevertheless, for a similar mean annual carbon (C) input, green manure and crop residues were more efficient in decreasing clay dispersivity and differential swelling whereas farmyard manure promoted SOC storage and was more efficient against slaking. QST curves had a strong discriminating power between reduced tillage and ploughing regardless of the indicator, as reduced tillage increases both total SOC content and root biomass in the topsoil.

The QST has several advantages. It (i) is rapid to run, (ii) doesn't require expensive equipment or consumables and (iii) provides a high density of information on both specific mechanisms of soil disaggregation and the overall soil structural stability. As an open access program for QST data management is currently under development, the test has a strong potential for adoption by a widespread community of end-users.

1 Introduction

Soil structure is one of the main factors controlling the fertility of temperate agricultural soils subject to intensive cultivation. REF? This is particularly true for Luvisols of the loess belt of Belgium, which are among the most productive soils of Europe and therefore have experienced a long cropping history. REF? The high productivity of these soils is primarily related to their high plant available water storage capacity as they are deep, stone-free and with a texture largely dominated by silt, up to 85 % in the topsoil. In addition, these soils which developed on Quaternary loess deposited $< 170.000\,\mathrm{years}$ ago (Antoine et al., 2003) still contain unweathered primary minerals in the subsoil, acting as a source of nutrients for plants (Vancampenhout et al., 2013). Their clay fraction is dominated by high activity clays, which provides a favourable cation exchange capacity for plant-available nutrient retention.

Since deforestation centuries ago, the chemical and biological fertility of these soils has increased over the course of cultivation, with topsoil pH, base saturation and earthworm activity increasing following repeated applications of organic and mineral fertilisers and amendments (Langohr, 2001). Nevertheless, today many of these soils have poor structural aggregate stability, which makes them particularly sensitive to physical damages such as compaction and erosion (Bielders et al., 2003). This structural weakness is related to a silt-dominated texture and enhanced by low soil organic matter (SOM) content in the topsoil. Between the 1960s and 2005, cropland soils of the loess belt of Belgium have lost $14\,\mathrm{tC\,ha^{-1}}$ on average, mainly caused by a shift from mixed crop-livestock farming systems towards arable farming systems, with a progressive disconnection from animal husbandry (Goidts and van Wesemael, 2007). This shift caused a decrease of farmyard manure application on cropland soil and a replacement of cereals and temporary grasslands by spring crops such as sugar beet, potato and chicory (Goidts and van Wesemael, 2007), thereby decreasing soil organic carbon (SOC) inputs. In parallel, the overall increase in ploughing depth, which dilutes ~~diluting~~ SOM vertically, has accentuated the decrease in SOC content in the topsoil layer (Meersmans et al., 2009). The Ap horizon of these soils has a typical SOC content of about $10\,\mathrm{g\,kg^{-1}}$ (Meersmans et al., 2011), which is clearly below the threshold value of $12\,\mathrm{g\,kg^{-1}}$ generally considered as critical for aggregate stability (Meersmans et al., 2011). The combination of a poor soil structural stability with an incomplete soil cover during the winter and spring periods (given the high proportion of spring crops in the rotation) increases erosion risks (Bielders et al., 2003), particularly under the growing risk of occurrence of extreme climatic events induced by climate change (IPCC, 2014).

In this agricultural context, conservation tillage appears as an effective way to decrease soil susceptibility to erosion and therefore has been increasingly adopted by farmers within the last 20 years. The replacement of moldboard ploughing by reduced tillage operations such as stubble cultivation has a positive effect on soil structure and water infiltration (Chabert and Sarthou, 2020; Holland, 2004), dramatically decreasing erosion risks (Seitz et al., 2019). Soil erosion is governed by both rainfall characteristics and environmental factors such as slope characteristics, soil cover as well as soil properties such as hydraulic conductivity and aggregate stability (Alewell et al., 2019; Maugnard et al., 2013). Owing to the difficulty to measure soil erosion and runoff, soil aggregate stability is often used as an indicator of soil erodibility (Barthès and Roose, 2002).

The process of soil aggregation is key to understanding understand the factors controlling soil aggregate stability. The theory of aggregate hierarchy of Hadas (1987) is widely accepted to conceptualise the internal organisation of soil aggregates. At the lowest level,

elementary clay plates ($< 2\,\mu m$) combine into clay floccules or domains, with a degree of organisation depending on clay mineralogy (quasi-crystals > domains > assemblage, Dexter, 1988). Domains combine into clusters ($2 - 20\,\mu m$) under the action of binding agents such as polyvalent cations (Al^{3+} strongly in acidic soils and Ca^{2+} and Mg^{2+} in neutral to slightly basic soils), Fe, Al and Mn oxides and organic compounds, mainly polysaccharides from bacterial and fungal mucilages or root exudates (Dexter, 1988; Tisdall and Oades, 1982). They can be very stable and contain organic acids or partially degraded bio-materials. These clusters combine into micro-aggregates $20 - 250\,\mu m$ in size (Edwards and Bremner, 1967; Six et al., 2004) that further combine into macro-aggregates ($> 250\,\mu m$) under the action of wetting and drying cycles (Dexter, 1988). Roots and fungal hyphae enmeshing micro-aggregates are recognised as critical binding agents in macro-aggregates, and are therefore influenced by soil management practices such as crop rotation and tillage (Tisdall and Oades, 1982). Clods ($> 25\,mm$) constitute the upper level of soil aggregation and are, in many agricultural soils, the result of compaction by agricultural machinery (Dexter, 1988). Under disaggregating forces, the destruction of one hierarchical order automatically destroys all higher hierarchical orders (Dexter, 1988).

Aggregate breakdown is controlled by four mechanisms (Le Bissonnais, 1996; Le Bissonnais and Le Souder, 1995): (i) Slaking occurs during fast-wetting of a soil and consists in the fragmentation of macro-aggregates into micro-aggregates by internal pressure exerted by air entrapment in soil porosity. (ii) Mechanical breakdown by raindrop impact, also known as splash erosion, initiates soil sealing and crusting by liberating elementary particles from soil aggregates. Its amplitude relies magnitude depends on raindrop characteristics as well as on internal soil cohesion, which decreases logarithmically with increasing water content (Dexter, 1988). The resistance of soil to mechanical breakdown also improves resistance to soil compaction due to traffic on the field. REF (iii) The breakdown by differential swelling occurs under wet conditions and depends on both the abundance and swelling properties of clay particles in soil. Nevertheless, this process mainly plays a role at macroscopic scale and has therefore a limited effect on soil disaggregation relative to the other mechanisms (Le Bissonnais, 1996). (iv) Physico-chemical or clay dispersion is the last mechanism, occurring when soil is wet. Clay dispersion depends on the ionic status of the soil (ionic strength in soil solution and the exchangeable sodium percentage) as well as the mineralogy of clays. Clay dispersion jeopardises the smallest level of soil aggregation (namely quasi-crystals, domains or assemblages of clay particles) to liberate elementary particles, which deteriorates any upper level of soil aggregation (Dexter, 1988).

A large number of laboratory methods exist for the measurement of soil aggregate stability. Traditional methods are destructive and rely on the resistance of soil aggregates to fragmentation under wet or, less often, dry conditions. Some wet fragmentation methods rely on the disaggregating power of the wetting treatment only, such as percolation stability (e.g., Mbagwu and Auerswald, 1999; Wuddivira et al., 2009), high Energy Moisture Content (e.g., Levy and Mamedov, 2002), or fast and slow wetting (e.g., Le Bissonnais, 1996). Other methods in wet conditions rely on an additional energy input, such as wet sieving methods (e.g., Hénin et al., 1958; Kemper and Rosenau, 1986; Yoder, 1936), those involving shaking or ultrasonication for clay dispersion (e.g., Haynes, 1993; Zhu et al., 2016), disaggregation by raindrop impact (e.g., Imeson and Vis, 1984) or rainfall simulators (e.g., Loch, 1989).

Recently, the SLAKES mobile application provided encouraging results as a tool for rapid data acquisition on soil structure. The test relies on image recognition to measure the increase in area of a soil aggregate as it disperses in water (Bagnall and

Morgan, 2021; Fajardo et al., 2016; Jones et al., 2021). The potential of some non-destructive methods ~~on~~ for the evaluation of soil structure and aggregation has also been revealed, such as aggregate delineation by analysis of X-ray microtomography images (Koestel et al., 2021), or aggregate stability prediction by visible-near infrared (VIS-NIR) spectroscopy (Shi et al., 2020).

The multiplicity of methods highlights how challenging ~~is~~ the measurement of soil aggregate stability is. From one study to another, the preferred approach is a matter of compromise depending on (i) the objective of the work (evaluation of soil structure, management of erosion or compaction risks), (ii) local conditions of soil, topography, climate and cropping (the drivers of erosion or compaction risks), (iii) the technicality, cost and delay of measurement; and (iv) the spatial scale of the soil unit to investigate.

In this work, we evaluated the performance of a new, simple test to measure soil structural stability, named QuantiSlakeTest (QST). It is a quantitative approach of the slake test, a visual qualitative test to illustrate the impact of soil management practices on soil structure. It consists in the dynamic weighing of a structured soil sample suspended in demineralised water. This approach has the advantage of being simple, rapid and dynamic, therefore providing a high density of information throughout the process of soil wetting and disaggregation under water.

The objective of this work was threefold: we aimed to (i) unravel the mechanisms controlling ~~soil mass evolution under water~~ the change in soil mass upon immersion in water and derive indicators from the QST curves to evaluate soil structural stability; (ii) investigate the relationship between soil properties and QST indicators, particularly SOC and clay contents; and (iii) assess how QST indicators respond to contrasting soil management practices.

To meet these goals, we sampled the soil of 35 plots from three long-term field trials of the Walloon agricultural research centre (*Centre wallon de recherches agronomiques*, CRA-W) dealing respectively with contrasting practices of organic matter (OM) inputs, tillage and P-K fertilisation. For each plot, we compared the QST indicators to the mean weight diameters (MWD) and the percentage of macro-aggregates (MA, $> 200\,\mu m$) from the three tests of Le Bissonnais (1996), used as a reference method.

2 Materials and methods

2.1 Description of the field trials

The soils under study have been subject to contrasting soil management practices ~~for a long time~~ in three long-term field experiments dealing with soil tillage, organic matter inputs and P-K mineral fertilisation, respectively. All trials are located on the agricultural station of the CRA-W in Gembloux, a town in the centre of the silt loam region of Wallonia, southern Belgium. The climate is oceanic temperate, with a mean annual temperature of $10.2°C$ and a mean annual rainfall of $793\,mm$ for the 1991-2020 period[1]. All soils are developed from loess, a silt-dominated unconsolidated and stone-free Quaternary sediment (Antoine et al., 2003). Soils are classified as hortic Luvisols according to the WRB (IUSS Working Group WRB, 2014). In April 2019, when the soil sampling was carried out, the three trials were covered with winter wheat (*Triticum aestivum*).

[1] https://www.meteo.be/resources/climatology/climateCity/pdf/climate_INS92142_9120_fr.pdf

2.1.1 Organic matter trial

The organic matter trial (OM trial, $50.560°$ N, $4.726°$ E) was set up in 1959, with the initial goal of addressing the issue of decreasing organic matter inputs (farmyard manure, crop by-products) on cropland soils of the silt loam region and related consequences on soil properties, crop yields and farm profitability (Roisin, 2018). The trial includes six contrasting treatments of SOM restitution in plots of $70\,\mathrm{m} \times 10\,\mathrm{m}$, repeated six times, following a Latin square design with the blocks aligned in a row. From 1959 to 1974, the field was cropped according to a four-year rotation with sugar beet (*Beta vulgaris*) as the starter crop, followed by three years of winter cereals – wheat, oat (*Avena sativa*), barley (*Hordeum vulgare*) – or two winter cereals – wheat, barley/oat – and one legume – horsebean (*Vicia faba*). Cultivation cycle shifted from 1975 onwards to a three-year sugar beet – winter wheat – winter barley rotation. Among the six treatments, three were selected for soil sampling in 18 plots, described by Buysse et al. (2013b). The 'residue exportation' (RE) treatment consists in a maximal exportation of by-products (straws and sugar beet heads and leaves) and no farmyard manure application nor green manure during the intercropping period. Since 2009 however, sugar beet heads and leaves are left on the field. The 'farmyard manure' (FYM) treatment consists in one application of 30 to $60\,\mathrm{tons\,ha^{-1}}$ of composted cattle manure once per rotation, after the harvest of the winter barley in order to enrich the soil for the sugar beet. The last application before soil sampling occurred on the 26th of July 2017. In the 'residue restitution' (RR) treatment, all crop by-products (cereal straws and sugar beet heads and leaves) are left on the fields, and one cover crop acting as a green manure is sown once per rotation during the intercropping period between the winter barley and the sugar beet. Cover crops were vetches (*Vicia sp.*) until 2009, except (i) mustard (*Sinapis alba*) in 1980, (ii) phacelia (*Phacelia sp.*) in 2011 and 2014 and (iii) mix of oat, vetch and clover (*Trifolium sp.*) in 2017. The estimated annual total carbon (C) input amounts to $315 \pm 76\,\mathrm{gC\,m^{-2}}$, $472 \pm 82\,\mathrm{gC\,m^{-2}}$ and $487 \pm 93\,\mathrm{gC\,m^{-2}}$ for the RE, FYM and RR treatments, respectively (Buysse et al., 2013a). Since the start of the trial, yearly measurements of topsoil properties ($0 - 25\,\mathrm{cm}$) show a drop of SOC content for the RE treatment, an increase for the FYM treatment and a steady state for the RR treatment (Buysse et al., 2013b). For all treatments, the soil has been ploughed annually with a moldboard plough.

2.1.2 Tillage trial

The soil tillage trial ($50.560°$ N, $4.727°$ E) was set up in 2004 and follows a two-year rotation of winter wheat and a spring crop, generally sugar beet or flax (*Linum usitatissimum*), with an exception in 2018 where corn (*Zea mays L.*) was cultivated as spring crop. A green manure is sown after tillage following the harvest of the cereal and destroyed during winter time before the spring crop. The trial includes four tillage treatments in plots of $24\,\mathrm{m} \times 21.5\,\mathrm{m}$ repeated four times, following a Latin square design with the blocks aligned in a row. Among the four treatments, the two most contrasting ones were sampled in eight plots: (i) annual ploughing (P) to a depth of $25 - 30\,\mathrm{cm}$ with a moldboard plough; (ii) annual reduced tillage (RT) with a spring tine cultivator tilling to a depth of about $10\,\mathrm{cm}$.

2.1.3 P-K mineral fertiliser trial

The P-K mineral fertiliser trial ($50.582°$ N, $4.687°$ E) was set up in 1967, with the initial goal of assessing the effect of the rate of P and K mineral fertiliser application on crop quality and yield, nutrient exportation with harvest, soil properties and farm profitability (Roisin, 2019). The trial comprises three levels of phosphorus (P) fertiliser (applied as superphosphate $18\,\%$ or triple superphosphate $45\,\%$) crossed with three levels of potassium (K) fertiliser (applied as KCl 40 or $60\,\%$), namely nine different treatments repeated three times in two randomized complete blocks, for a total of 54 plots of $7.5\,\mathrm{m} \times 50\,\mathrm{m}$. The lower level of P and K fertilisation received no P and K mineral fertiliser since 1975 (P0 and K0). The intermediate level of fertilisation consists in balancing P and K outputs and inputs, according to the nutrient balance method (P1 and K1). The higher level of fertilisation is over-fertilised, multiplying by 2 (until 2000) or 1.5 (onwards) the amount of P and K applied to the P1 and K1 treatments (P2 and K2). The last application of P-K fertilisers before soil sampling occurred on the 15 July 2016. The whole field is cropped according to a three-year rotation cycle similar to that of the organic matter trial, with sugar beet as starter crop followed by two winter cereals (winter wheat and winter barley). Since the start of the trial, the soil has not received any exogenous organic matter but all by-products (cereal straws and sugar beet heads and leaves) are left on the field to maintain sufficient SOC contents. For all treatments, soil is ploughed annually with a ~~classic~~ moldboard plough, except before the seeding of sugar beet in 2017 (soil was prepared by deep decompaction with a heavy tine cultivator at about $30\,\mathrm{cm}$ depth in august 2016). In this study, we focussed on the potential effect of contrasting levels of KCl application on soil structural stability (Paradelo et al., 2016). Therefore, we selected three repetitions of each level of K within the trial for soil sampling in 9 plots.

2.2 Soil sampling

Soils were sampled on the 8th and 10th of April 2019. For each of the 35 plots previously described, six structured soil samples of $100\,\mathrm{cm}^3$ were taken with steel Kopecky cylinders, in the inter-row, at a depth of $2 - 7\,\mathrm{cm}$. Soil was sampled in an area of $1\,\mathrm{m}^2$ that was sprayed three weeks earlier with about $32\,\mathrm{ml}$ of $10\,\mathrm{g\,l}^{-1}$ glyphosate, in order to stop plant growth and therefore standardise sampling conditions between plots at the time of sampling. Soils were carefully transported within the cylinders to the laboratory where they were unmoulded. For each plot, five samples were air-dried until constant weight for a period of about three months for QST analysis, whereas the last sample was dried at $105°\mathrm{C}$ and weighed for the determination of bulk density. Additionally to structured soil samples, about $2\,\mathrm{kg}$ of each soil was sampled at the same location and depth and gently crumbled by hand for the measurement of soil aggregate stability by the Le Bissonnais (1996) method and analysis of physico-chemical soil properties.

2.3 Soil analysis

2.3.1 Physico-chemical properties of soils

After homogenisation, about $500\,\mathrm{g}$ of each disturbed soil sample were gently crushed with a pie roll and sieved to $2\,\mathrm{mm}$, and the fraction $< 2\,\mathrm{mm}$ was sent to the *Centre interprovincial de l'agriculture et de la ruralité* in La Hulpe (Belgium) to be analysed. Soil pH was measured in water ($\mathrm{pH_{H_2O}}$) with a 1:5 soil:solution mass ratio, according to the norm NF-ISO-10390:2005 (International Organization for Standardization, 2005). Total C content was determined by dry combustion according to the norm NF-ISO-10694:1995 (International Organization for Standardization, 1995). Inorganic C content was measured by infrared quantification of $\mathrm{CO_2}$ emitted from soil after addition of orthophosphoric acid, according to the norm NF-EN-15936:2012 (Association Française de Normalisation, 2012). SOC content was calculated as the difference between total and inorganic C content. Soil texture (sand, silt and clay contents) was determined by sedimentation and sieving, according to Stokes law, by a method derived from the norm NF-X31-107:2003 (Association Française de Normalisation, 2003). Bulk density was measured from one structured soil sample per plot, dried at $105\,^{\circ}\mathrm{C}$ until constant weight, by dividing the mass of dry soil by the core volume ($100\,\mathrm{cm^3}$). The main properties of the soils of the experimental fields of the three trials are shown in the table 1 (open data available: https://doi.org/10.5281/zenodo.7405113).

2.3.2 Measurement of soil aggregate stability by *Le Bissonnais* method

Soil aggregate stability was measured according to the method of Le Bissonnais (1996), following the norm ISO-FDIS-10930:2011 (International Organization for Standardization, 2012). For each soil gently crumbled by hand, $5\,\mathrm{g}$ to $10\,\mathrm{g}$ of soil aggregates from 3 to $5\,\mathrm{mm}$ in size were subjected to three contrasting disaggregating treatments. The first test consists in fast-wetting soil aggregates in water, exacerbating the effect of slaking. The second test is a slow-wetting of soil aggregates by capillarity, to test their resistance to clay dispersion and differential swelling ~~under wet conditions~~ during wetting independently from the slaking effect. The third test consists in a standardised shaking of the aggregates in water after rewetting them in $95\,\%$ v/v ethanol for $30\,\mathrm{min}$, to test their mechanical strength while minimising slaking, differential swelling and dispersion. After each disaggregation treatment, the resulting aggregates were immersed in ethanol and dried at $40\,^{\circ}\mathrm{C}$ for $2\,\mathrm{hours}$. The size distribution of the remaining aggregates was measured by way of dry sieving, with sieves of $2\,\mathrm{mm}$, $1\,\mathrm{mm}$, $0.5\,\mathrm{mm}$, $0.2\,\mathrm{mm}$, $0.1\,\mathrm{mm}$ and $0.05\,\mathrm{mm}$.

Two main indicators were calculated from the fractions. The first is the mean weight diameter (MWD) of the aggregate fraction that survived each individual test, following the equation (International Organization for Standardization, 2012):

$$MWD = \frac{\sum(mean\ diameter\ between\ two\ sieves \times [weighed\ percentage\ of\ particles\ retained\ on\ the\ sieve])}{100} \quad (1)$$

The second indicator is the percentage of macro-aggregates (MA) remaining after each individual test, calculated as the mass fraction of soil aggregates $> 200\,\mu\mathrm{m}$.

Table 1. Soil properties of the 35 plots from the three long-term field trials. SOC = Soil Organic Carbon. The SOC:clay ratio was calculated for harmonised units for SOC and Clay, $\mathrm{g\,kg^{-1}}$. Open data available: https://doi.org/10.5281/zenodo.7405113

Plot	Treatment	Clay ($< 2\,\mu m$) %	Silt (2–50 μm) %	Sand (50–2000 μm) %	SOC $\mathrm{g\,kg^{-1}}$	SOC:clay [-]	$\mathrm{pH_{H_2O}}$ [-]	Bulk density $\mathrm{g\,cm^{-3}}$
Organic matter trial								
1	Farmyard manure	16.6	76.9	6.5	13.66	0.082	7.37	1.31
2	Farmyard manure	19.7	74.7	5.6	10.88	0.055	7.22	1.32
3	Farmyard manure	18.6	75.5	5.9	11.16	0.060	7.16	1.32
4	Residue exportation	16.1	77.5	6.4	8.82	0.055	7.07	1.28
5	Residue restitution	15.1	79.1	5.8	9.66	0.064	6.93	1.34
6	Residue restitution	14.8	78.8	6.4	9.84	0.067	6.86	1.30
7	Residue exportation	14.0	79.6	6.4	8.85	0.063	7.04	1.30
8	Farmyard manure	13.7	79.7	6.6	10.59	0.077	6.83	1.30
9	Residue exportation	15.8	78.0	6.2	8.80	0.056	6.88	1.34
10	Residue restitution	15.3	78.8	5.9	11.19	0.073	6.91	1.30
11	Residue restitution	18.9	75.6	5.6	9.84	0.052	6.99	1.32
12	Farmyard manure	15.3	78.5	6.2	10.22	0.067	6.75	1.36
13	Residue exportation	17.3	76.9	5.7	8.02	0.046	7.14	1.27
14	Farmyard manure	14.4	78.8	6.8	11.39	0.079	7.12	1.28
15	Residue restitution	17.1	76.9	6.0	9.81	0.057	6.98	1.30
16	Residue exportation	19.3	74.9	5.8	8.23	0.043	6.82	1.33
17	Residue restitution	19.0	75.4	5.5	9.36	0.049	7.08	1.32
18	Residue exportation	20.0	74.8	5.2	7.76	0.039	7.21	1.37
Tillage trial								
19	Reduced tillage	13.1	79.6	7.4	12.99	0.099	7.17	1.21
20	Ploughing	16.7	76.7	6.6	9.95	0.060	7.49	1.27
21	Reduced tillage	16.7	77.2	6.1	11.19	0.067	7.35	1.25
22	Ploughing	15.0	78.6	6.4	9.87	0.066	7.75	1.28
23	Ploughing	12.5	80.9	6.6	9.04	0.072	7.72	1.27
24	Reduced tillage	12.6	80.6	6.8	11.99	0.095	7.50	1.21
25	Ploughing	11.7	80.6	7.6	11.44	0.097	7.59	1.26
26	Reduced tillage	11.7	82.0	6.3	12.49	0.107	6.88	1.22
P-K mineral fertiliser trial								
27	P1 K0	19.9	74.9	5.3	11.92	0.060	6.86	1.28
28	P1 K1	20.0	74.2	5.8	9.75	0.049	6.91	1.31
29	P1 K2	19.9	74.2	6.0	11.40	0.057	7.00	1.30
30	P2 K1	16.2	77.7	6.1	10.83	0.067	6.61	1.35
31	P2 K0	15.0	78.3	6.7	11.52	0.077	6.95	1.25
32	P2 K2	16.6	77.5	5.8	11.74	0.071	6.80	1.39
33	P1 K2	16.9	78.1	5.0	12.50	0.074	6.85	1.33
34	P1 K0	12.8	81.0	6.2	11.03	0.086	6.69	1.28
35	P1 K1	13.0	81.6	5.4	9.69	0.074	6.69	1.27

The Le Bissonnais method has two main advantages : (i) the three tests target the three main mechanisms of soil disaggregation in field conditions, namely slaking, mechanical breakdown and clay dispersion differential swelling - and (ii) it measures the size distribution of particles remaining after the disaggregation treatment, which provides further insight in soil susceptibility to water erosion (Le Bissonnais, 1996).

2.3.3 Soil structural stability measurement by the QuantiSlakeTest (QST) method

Whereas Le Bissonnais (1996) and other reference methods measure the stability of soil aggregates of a few mm in size, the QST works on 100 cm³ soil volumes rather than on soil aggregates. Accordingly, we consider that referring to 'soil structural stability' rather than 'soil aggregate stability' is more correct when referring to QST measurements, and we will therefore stick to "soil structural stability" for QST measures.

The QST method consists in plunging an undisturbed soil sample supported by an $8\,\mathrm{mm}$ metallic mesh basket into demineralised water, and measuring soil mass continuously using the underfloor weighing hook of the balance. The balance is connected to a computer for data logging (Fig. 1). For each plot, the five air-dried structured soil samples were left to slake for approximately $1000\,\mathrm{sec}$ (around $17\,\mathrm{min}$), with recording time step ~~frequency~~ decreasing from less than one second at the start of the experiment to approximately $30\,\mathrm{s}$ at the end. Due to some electronic or computer issues during the experiment, some samples were lost. In total, the data from 157 QST curves could be processed and constituted the main database of our study. Most of the 35 plots had five or four usable QST curves (20 and 13 plots respectively). One plot from the OM trial and one from the P-K mineral fertiliser trial had only three and two usable curves, respectively.

Immediately after soil immersion in water, the soil mass drops due to Archimedes' upward buoyant force (Fig. 2). The general shape of one QST curve is presented in Fig. 3, as well as the main indicators that have been calculated from the curves. The first ~~value~~ record of soil mass under water is defined as ~~the~~ time 0 (t_0) of the QST approach (Fig. 3). In the initial phase, soil mass generally increases due to water filling the porosity. After a few seconds or minutes, the soil mass reaches a maximum (W_{max} at t_{max}) before decreasing~~,~~ once mass loss due to disaggregation becomes dominant compared to mass gain by wetting. Soil mass was normalised ~~according~~ relative to W_{max} ($\mathrm{W\,max} = 1[-]$), so that mass values are relative soil masses, varying between 0 and 1.

QST indicators calculated from the QST curves were split into four categories (Fig.3) :

- (i) indicators related to the early increase in soil mass soon after soil immersion in water; they include the time to reach the maximum mass value (t_{max}); the increase in soil mass between t_0 and t_{max} (W_{max}-W_{t0}); and the slope between t_0 and t_{max} ($Slope_{0\text{-}max}$);
- (ii) indicators related to slopes in the decreasing part of the curve, at different timesteps (after $30\,\mathrm{s}$, $60\,\mathrm{s}$, $300\,\mathrm{s}$ and $600\,\mathrm{s}$) in the decreasing part of the curve, taking t_{max} as the starting point ($Slope_{max\text{-}30}$, $Slope_{max\text{-}60}$, $Slope_{max\text{-}300}$ and $Slope_{max\text{-}600}$). Local slopes were also calculated between $30\,\mathrm{s}$ and $60\,\mathrm{s}$ ($Slope_{30\text{-}60}$), between $60\,\mathrm{s}$ and $300\,\mathrm{s}$ ($Slope_{60\text{-}300}$) and between $300\,\mathrm{s}$ and $600\,\mathrm{s}$ ($Slope_{300\text{-}600}$);
- (iii) indicators linked to threshold values of mass loss. They correspond to the time needed to reach a certain fraction of relative mass loss between the maximum and the final mass of soil at the end of the QST experiment. Threshold

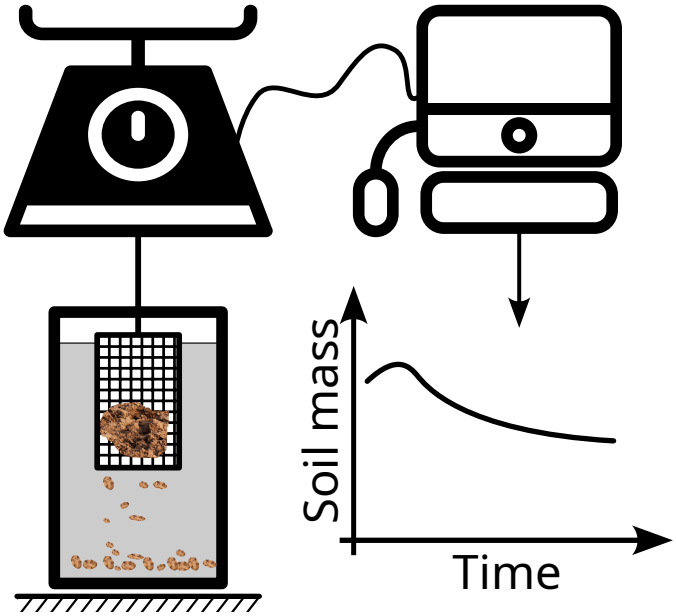

Figure 1. The QuantiSlakeTest (QST) aims ~~in~~ at weighing an undisturbed soil sample suspended ~~into~~ in demineralised water by means of an 8 mm mesh metallic basket. The QST device, illustrated here, consists in a balance connected to a computer for direct data-logging. The open-source application for parameterising and driving the experience and for visualising data is released as a development R-package (<https://frdvnw.gitlab.io/slaker/dev/>). Video comparing the QST of two contrasting soil samples can be watched here: <https://youtu.be/G9UweThvHYI> – Credits : figure based on two illustrations by Adnen Kadri from the Noun Project.

values of 25, 50, 75, 90 and 95 % of relative mass loss were calculated (t25, t50, t75, t90 and t95). The time between two threshold values of mass loss were also calculated ($dt_{max\text{-}25}$, $dt_{25\text{-}50}$, $dt_{50\text{-}75}$, $dt_{75\text{-}90}$ and $dt_{90\text{-}95}$). *Nota bene* - $t25=dt_{max\text{-}25}$, $dt_{max\text{-}25}$ will be used in the following manuscript, tables and figures ;

– (iv) global indicators providing ~~a complete~~ an integrative overview of soil mass evolution all over the QST. They include relative soil mass at the end of the experiment (W_{end}) and the Area Under Curve (AUC). For these two indicators, a reference time of 900 s was considered;

2.3.4 Measurement of root biomass after slaking

For samples from the soil tillage trial, root biomass retained in the metallic basket were weighed after running the QST by cleaning remaining soil with a water jet. The roots were dried carefully with a Tork paper, air-dried and weighed.

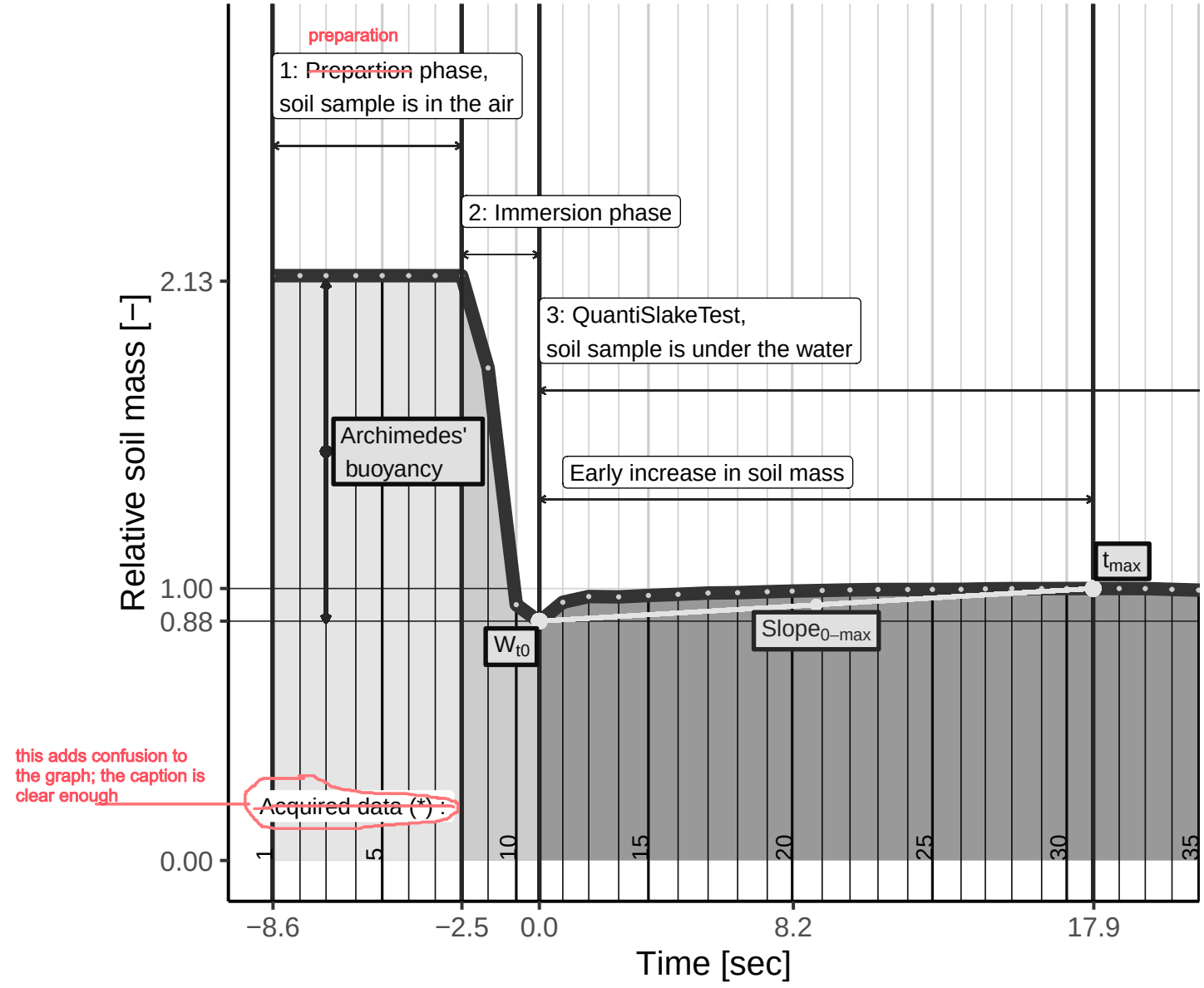

Figure 2. Early phases of the QST, before and during the immersion of the soil sample. The Archimedes' buoyancy appears clearly between the first phase (preparation of the QST) and the beginning of the third phase (the QST in itself). Mathematical functions are used for automatically identified the starting of the test, based on first-order and second-order derivatives. The early increase in soil mass is only slightly visible at this scale. ~~(*)~~ Each vertical line represents one pair of data (time and weight) acquired by the computer, i.e. one line of the raw data file.

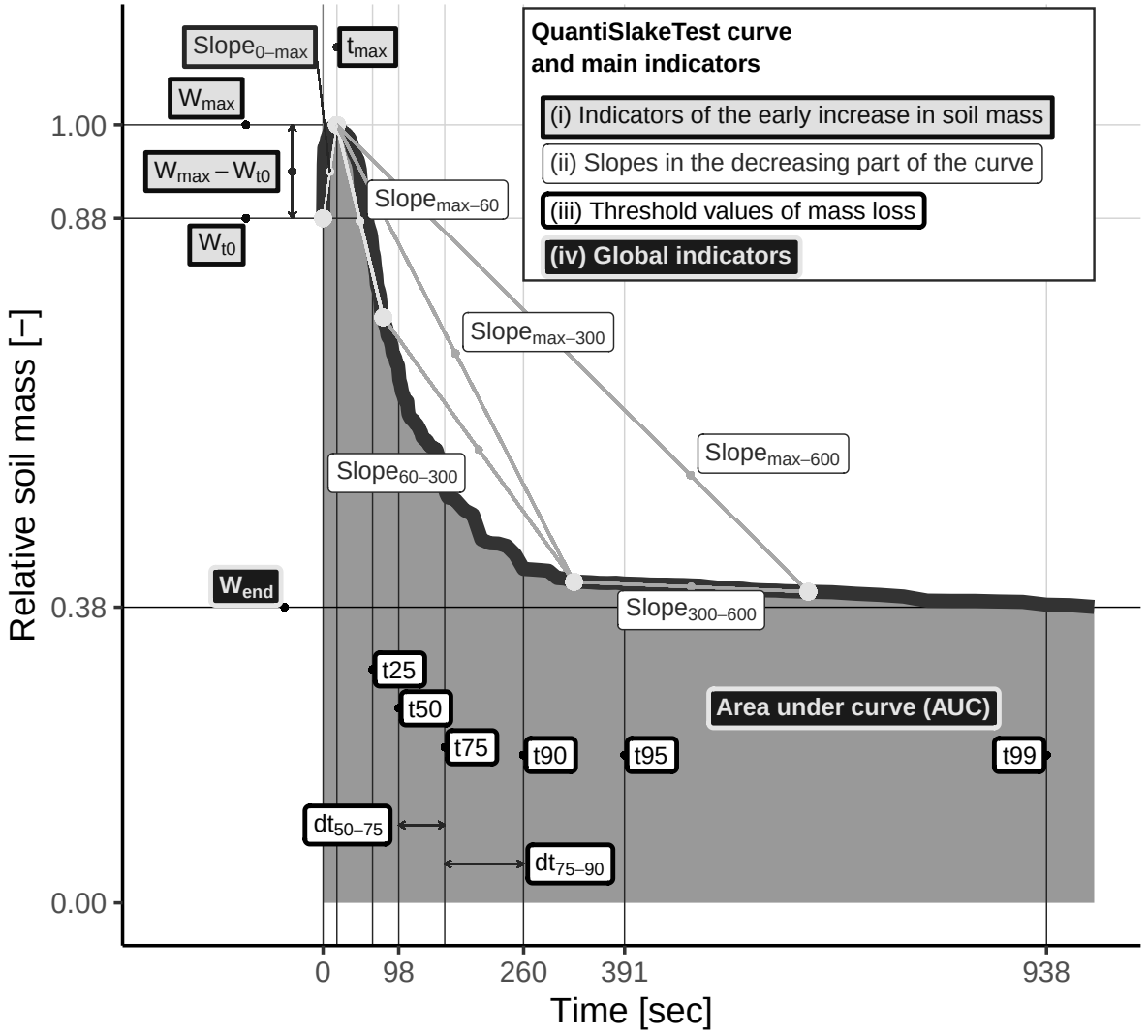

Figure 3. Main parameters ~~are~~ derived from a QST curve. (i) Inside thick square light grey boxes (upper left), indicators related to the early increase in soil mass including time to reach the maximum mass value (t_{max}); the increase in soil mass between t_0 and t_{max} (W_{max}-W_{t0}); and the slope between t_0 and t_{max} ($Slope_{t0\text{-}max}$). (ii) In thin round white boxes (upper right), slopes at different time steps (after 60 s, 300 s and 600 s) in the decreasing part of the curve, taking t_{max} as the starting point ($Slope_{max\text{-}60}$, $Slope_{max\text{-}300}$ and $Slope_{max\text{-}600}$) or between these time steps ($Slope_{60\text{-}300}$ and $Slope_{300\text{-}600}$). (iii) In thick round white boxes (below the curve), time needed to achieve 25, 50, 75, 90,95 and 99% of relative mass loss (t25, t50, t75, t90, t95 and t99) and between thresholds ($dt_{50\text{-}75}$ and $dt_{75\text{-}90}$). And finally, (iv) in black boxes, the two global indicators including sample relative mass at the end of the experiment (W_{end}) and the Area Under Curve (AUC, shaded area). For the sake of clarity, not all calculated indicators are shown here. For this illustration, ~~the~~ data from a real QST done on a sample from plot 29 of the P-K mineral fertiliser trial (see table 1)

was used

2.3.5 Data analysis

Between continuous variables, correlation coefficients were determined. For QST indicators, average values were calculated at the plot level for comparison with data that were measured only at the plot level: aggregate stability indicators from Le Bissonnais and physico-chemical soil properties. Since many QST indicators are calculated from ~~one~~ the same curve, a correlation matrix was drawn for QST indicators, to evaluate the level of redundancy between them and propose a selection to be used for the statistical analysis of soil management practices in the long-term experiments.

In order to test whether soil management practices affect QST indicators, Linear Mixed-Effects Models were fitted and tested by analysis of variance (ANOVA). For each test, the QST indicator was used as the outcome variable and the treatments of the trials were used as a fixed explanatory variable, whereas the blocks were defined as a random effect. As several samples were related to one single plot (157 QST in total from 35 plots), the plot identifier was added as a random effect of the model to take into account the dependence between field replicates from one plot.

Prior to the ANOVA, the normality and the homoscedasticity of the residuals of the models were verified using respectively Shapiro-Wilk and Bartlett tests. For all the models, the significance of differences in QST indicators between soil management practices were tested using classical analysis of variance (ANOVA, Type II Wald F tests with Kenward-Roger estimation of degree of freedom, Fox and Weisberg, 2019). When the F-test was significant ($p < 0.05$), post-hoc comparisons were performed: treatments of the trial were compared pairwise at 0.05 probability level of significance using estimated marginal means (EMMs, also named least-squares means, Lenth, 2022).

All statistical analyses were performed using R version 4.3.0 (2023-04-21) software (R Core Team, 2023). The linear mixed-effect models were performed with the lme4 package (Bates et al., 2015), the ANOVA with the car package (Fox and Weisberg, 2019) and contrast analyses with the emmeans package (Lenth, 2022).

3 Results

3.1 Redundancy analysis

The correlation matrix of QST indicators is presented in Appendix, in table A1. From this table, it appears that several indicators are strongly positively correlated. A high level of redundancy ($r > 0.9$) exists between:

- W_{end}, AUC, $Slope_{max\text{-}300}$ and $Slope_{max\text{-}600}$
- $Slope_{max\text{-}30}$ and $Slope_{max\text{-}60}$
- t_{max}, $dt_{max\text{-}25}$ and t50
- t50 and t75, t75 and t90, t90 and t95
- various dt and t (e.g.: $dt_{25\text{-}50}$ and t50, $dt_{50\text{-}75}$ and t75)

Accordingly, to limit redundancy, the output of the statistical analysis of QST indicators against soil management practices was limited to four QST indicators selected according to the following criteria: - One indicator was chosen for each category

previously defined in the methods (i - early increase in soil mass; ii - early to intermediate mass loss; iii – intermediate to late mass loss; and iv - global indicators) - The use of highly redundant indicators ($r > 0.7$) was avoided. - In the same category of indicator, most discriminant indicators between soil management practices was chosen. If arbitration between two was necessary, the conceptually simplest one was kept.

Fig. 3

indicators

the indicator was chose that allowed to best discriminate among management practices

According to these decision rules, we focused on (i) t_{max}, (ii) $Slope_{30-60}$ (for the tillage & PK trial) or $Slope_{60-300}$ (for the SOM trial), (iii) dt_{50-75} and (iv) W_{end}

3.2 Comparison of QST indicators with Le Bissonnais

Except for the $Slope_{0-max}$, a positive correlation was found between all QST indicators and the mean weight diameter (MWD1) and the percentage of macro-aggregates (MA1) of the fast wetting test of Le Bissonnais (Table 2). The higher correlation coefficients were found for QST indicators related to the early stages of the curve (t_{max}, W_{max}-W_{t0}, $Slope_{max-30}$, $Slope_{max-60}$, dt_{max-25} and t50). Correlation decreases progressively for later slopes ($Slope_{max-300}$, $Slope_{max-600}$) as well as for t75 to t95 and is minimal for sample residual mass at the end of the test (W_{end}). Similarly, the mean weight diameters (MWD2) of the slow wetting test of Le Bissonnais also correlate positively with each QST indicator except $Slope_{0-max}$. However, correlations tend to increase for QST indicators related to the intermediate to late stage of the curve, particularly t50 to t95 and dt_{max-25}, dt_{25-50} and dt_{50-75} (Table 2). In contrast to the fast wetting test, the percentage of macro-aggregates surviving the slow wetting (MA2) are poorly related to QST indicators. For the third test of Le Bissonnais, testing soil resistance to mechanical breakdown, mean weight diameter (MWD3) correlates poorly with QST indicators. Similarly, correlation between QST indicators and the percentage of macro-aggregates surviving the third test (MA3) is always negative and generally poor, except for W_{max}-W_{t0} (r=-0.60, Table 2). Regardless of the test, sample mass at the end of the experiment (W_{end}) correlates poorly with MWDs from Le Bissonnais, considered alone or in combination (data not shown). Correlation between the area under curve (AUC) and MWD1 (r=0.41) and MWD2 (r=0.38) is a bit higher but remains poor.

3.3 Soil aggregate and structural stability against soil properties

3.3.1 Le Bissonnais

The correlation matrix between Le Bissonnais' indicators and soil properties is shown in Appendix, in table A2. A positive correlation exists between total SOC content and both MWD1 (r=0.75) and MWD2 (r=0.70), whereas MWD3 and MA3 correlate poorly with SOC content (r=0.11 and -0.07, respectively). In contrast, clay content correlates positively with MWD3 and MA3 (r=0.52 and 0.66, respectively) but poorly with MWD1 and MWD2 (r=-0.35 and -0.12). Linear relationship with the SOC:clay ratio, evidenced as a proxy for predicting field soil structural quality by visual assessment methods (Johannes et al., 2017) was also tested. The SOC:clay ratio correlated positively with both MWD1 (r=0.67) and MWD2 (r=0.48) and negatively with MWD3 (r=-0.33) and MA3 (r=-0.55). No clear linear relationship was found between Le Bissonnais' indicators and pH or bulk density.

Table 2. Correlation coefficients between QST indicators calculated from individual curves, Mean Weight Diameters (MWD) and percentages of macro-aggregates (MA) from the three tests of Le Bissonnais (1. Fast wetting; 2. Slow wetting; 3. Mechanical breakdown) and soil properties. The gradient of colours relates to the positive (blue) or to the negative (orange) relative amplitude of correlation coefficients.

	Le Bissonnais *et al.* (1996)						Soil properties				
	MWD 1	MWD 2	MWD 3	MA 1	MA 2	MA 3	SOC	Clay	SOC:Clay	pH	Bulk density
(i) QST indicators of the early increase in soil mass											
Slope 0-max	-0.12	-0.15	0.09	-0.19	0.06	0.32	-0.03	0.39	-0.34	-0.08	0.09
tmax	0.60	0.51	-0.26	0.57	-0.06	-0.46	0.52	-0.67	0.82	0.03	-0.49
Wmax-Wt0	0.58	0.36	-0.37	0.57	-0.12	-0.60	0.56	-0.83	0.92	0.08	-0.61
(ii) QST slopes in the decreasing part of the curve											
Slope max-30	0.47	0.37	-0.16	0.48	0.02	-0.36	0.41	-0.64	0.67	-0.03	-0.14
Slope 30-60	0.48	0.50	0.11	0.38	0.09	-0.09	0.38	-0.33	0.49	-0.20	-0.28
Slope 60-300	-0.10	-0.04	0.17	-0.20	-0.27	-0.02	-0.18	-0.11	0.02	0.19	-0.42
Slope 300-600	-0.33	-0.45	-0.04	-0.29	-0.23	0.00	-0.37	0.07	-0.25	0.09	-0.13
(iii) QST threshold values of mass loss											
dt max-25	0.60	0.50	-0.18	0.57	0.04	-0.32	0.52	-0.51	0.68	-0.08	-0.18
dt 25-50	0.49	0.57	-0.07	0.41	0.10	-0.21	0.43	-0.29	0.52	-0.01	-0.23
dt 50-75	0.38	0.68	-0.01	0.32	0.20	-0.14	0.47	-0.23	0.49	0.05	-0.32
dt 75-90	0.25	0.36	-0.08	0.23	0.14	-0.24	0.32	-0.27	0.44	0.09	-0.26
t50	0.57	0.56	-0.13	0.52	0.07	-0.28	0.50	-0.43	0.63	-0.05	-0.21
t75	0.49	0.66	-0.06	0.43	0.15	-0.21	0.51	-0.33	0.58	0.01	-0.29
t90	0.43	0.59	-0.08	0.38	0.16	-0.25	0.48	-0.34	0.58	0.05	-0.31
t95	0.39	0.64	-0.09	0.36	0.22	-0.27	0.55	-0.35	0.61	0.15	-0.34
(iv) QST global indicators											
Wend	0.33	0.27	0.03	0.26	-0.17	-0.25	0.20	-0.54	0.53	0.00	-0.39
AUC	0.41	0.38	0.01	0.35	-0.10	-0.28	0.30	-0.58	0.61	-0.01	-0.38

3.3.2 QuantiSlakeTest

Generally, indicators derived from QST curves correlate positively with SOC content, except for $Slope_{0\text{-}max}$ and $Slope_{60\text{-}300}$ and $Slope_{300\text{-}600}$. Coefficients remain low to moderate though, with the stronger coefficient obtained for W_{max}-W_{t0} (r=0.56) and t95 (r=0.55) (Table 2). In contrast, most QST indicators correlate negatively with clay content. The stronger coefficients were found for W_{max}-W_{t0} (r=-0.83), t_{max} (r=-0.67), $Slope_{max\text{-}30}$ (r=-0.64) and AUC (r=-0.58) (Table 2). This antagonist effect of SOC and clay contents on soil resistance to disaggregation under water is well captured by the SOC:clay ratio, which correlates strongly with indicators from the start of QST curves, particularly W_{max}-W_{t0} (r=0.92, Table 2 and detailed in Fig. 4) but also t_{max} (r=0.82), $Slope_{max\text{-}30}$ (r=0.67) and $dt_{max\text{-}25}$ (r=0.68). While we observe a clear relationships between W_{max}-W_{t0} and SOC:clay ratio (Fig. 4) we observe a residual variability in the repeated test of a same plot, that could be explained by local soil conditions of the sampling sites (eg. slopes, presence of roots, or earthworms' galleries).

Similarly to indicators of soil aggregate stability from Le Bissonnais, all indicators from the QST curves correlated poorly with pH. Except for $Slope_{0\text{-}max}$, a moderate to poor negative correlation is observed between QST indicators and bulk density, with the lower values obtained for W_{max}-W_{t0} (r=-0.61) and t_{max} (r=-0.49).

3.4 Soil structural stability under contrasting soil management practices

The responses of soil structural stability indicators calculated from QST curves to contrasting long-term soil management practices from the three long-term experiments are presented in this section. As mentioned previously ~~For the sake of clarity and to limit redundancy,~~ we have focused on a selection of four indicators: (i) t_{max}, (ii) $Slope_{30\text{-}60}$ for the tillage & PK trial or $Slope_{60\text{-}300}$ for the SOM trial, (iii) $dt_{50\text{-}75}$ and (iv) W_{end}, ~~one for each category defined in the methods: (i) early increase in soil mass, (ii) slopes in the decreasing part of the curve, (iii) threshold values of mass loss and (iv) global indicators.~~

3.4.1 Organic matter trial

Soils of the three treatments of OM inputs in the OM trial have different contents of total SOC, with the FYM treatment having the highest SOC content ($11.32\,g\,kg^{-1}$), the RE treatment having the lowest SOC content ($8.41\,g\,kg^{-1}$) and the RR treatment having an intermediate value ($9.95\,g\,kg^{-1}$). Accordingly, t_{max} tends to respect this gradient of total SOC, with the FYM showing the best scores on average ($p = 0.047$, Fig. 5a-d). Counter-intuitively though, this order is not respected anymore for QST indicators related to intermediate or late stages of the curves ($Slope_{60\text{-}300}$, W_{end}). The response of treatments follows the order RR > RE > FYM for $Slope_{60\text{-}300}$ ($p = 0.005$, Fig. 5c) and for W_{end} ($p = 0.098$, Fig. 5d). Discordant results were also obtained between the three tests of Le Bissonnais, with the MWD scores from the fast wetting test (MWD1) slightly in favour of the FYM treatment (FYM ~ RR > RE; n.s., results in Appendix, Fig. B1) and the scores from the slow wetting test (MWD2, n.s.) and from the mechanical breakdown (MWD3, $p < 0.05$) in favour of the RR treatment (RR > FYM ~ RE; results in Appendix, Fig. B1).

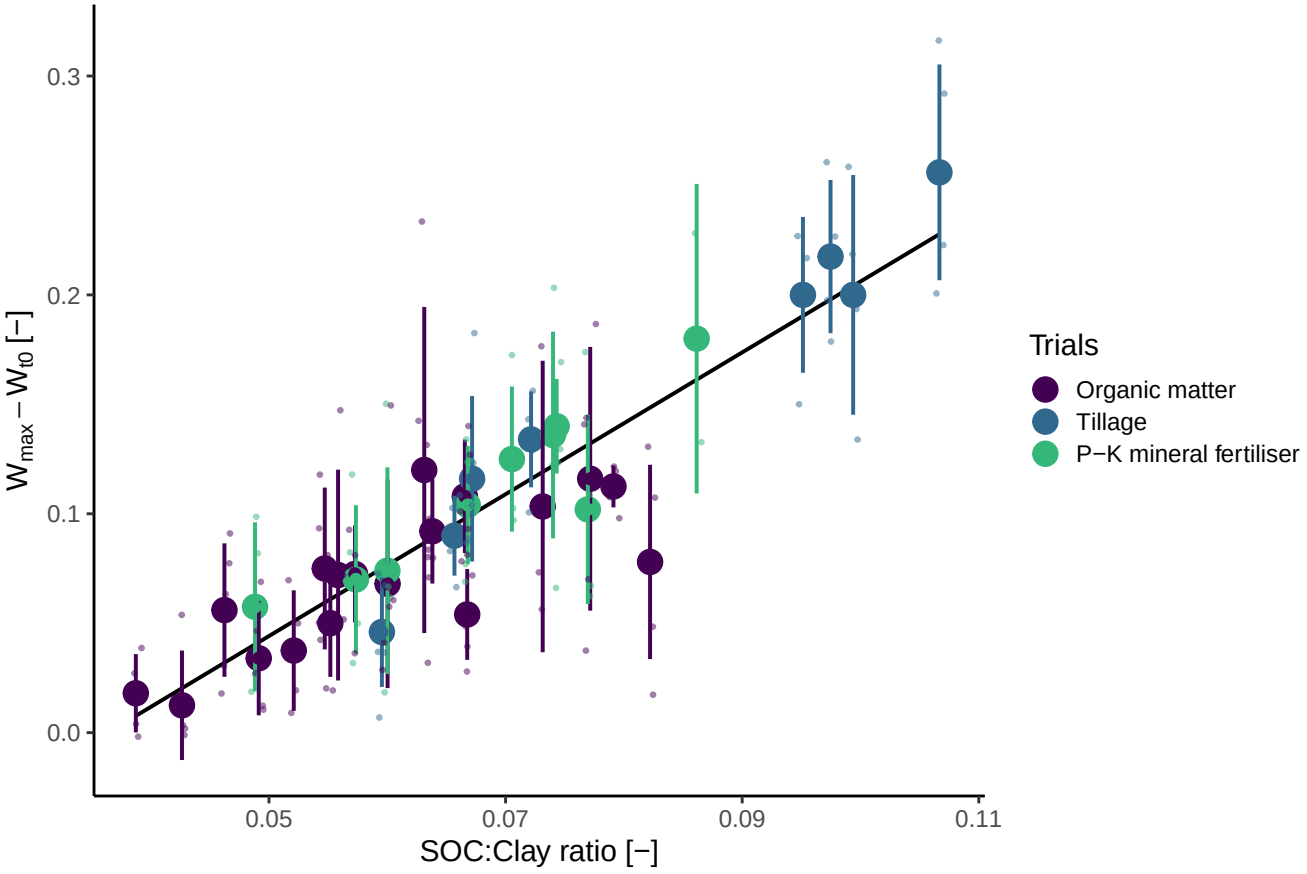

Figure 4. Early increase in soil mass under water measured from QST curves (W_{max}-W_{t0}) against the SOC:clay ratio of bulk soil (r=0.92). Small dots are individual QST indicator with a small amount of noise added in x. Large dots are the mean and bars are standard deviation by plot.

3.4.2 Tillage trial

Remarkably, the QST responds very well to contrasting tillage treatments, with all QST indicators having a better score for reduced tillage (RT) than for ploughing (P) (Fig. 6 and Fig. 7). This result is in agreement with total SOC content, RT having an average SOC content of $12.16\,\mathrm{g\,kg^{-1}}$ whereas P treatments have an average SOC content of $10.07\,\mathrm{g\,kg^{-1}}$. Similarly, a higher root biomass content was measured in the topsoil under RT, with $42 \pm 19\,\mathrm{mg}$ of root biomass for the RT treatment against $31 \pm 16\,\mathrm{mg}$ for the P treatment (p=0.168). However, Slope~30-60 ($p < 0.007$) and W_{end} ($p < 0.008$) are more sensitive to tillage than t_{max} and $dt_{50\text{-}75}$ (Fig. 7). Indicators from the three tests of Le Bissonnais provide similar results, with the most contrasting response between RT and P tillage treatments obtained for the fast wetting test (Appendix, Fig. B2). However, $Slope_{30\text{-}60}$ and W_{end} discriminate better between tillage treatments than MWD1 ($p < 0.05$).

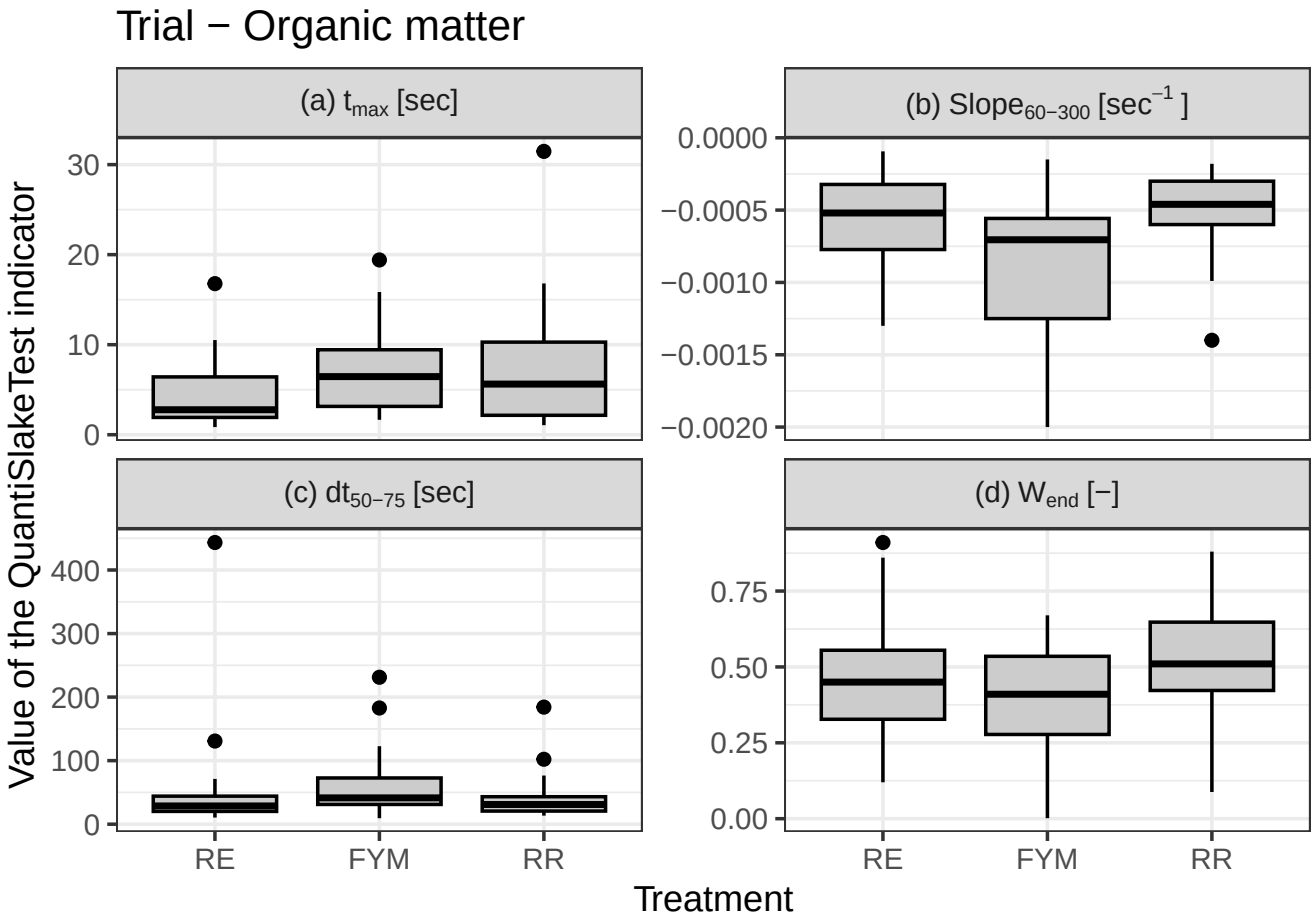

Figure 5. Boxplots of four QST indicators against treatments of OM input for the soils from the organic matter trial, 'residue exportation' (RE), 'farmyard manure' (FYM) and 'residue restitution' (RR). a) t_{max}; b) $Slope_{60-300}$; c) dt_{50-75} ; d) W_{end}.

3.4.3 P-K mineral fertiliser trial

follows

In the P-K mineral fertiliser trial, soil structural stability ~~respects~~ the order K2 > K0 > K1 regardless of the QST indicator (data not shown), but without any significant differences (n.s.). Similar results were obtained with the three tests of Le Bissonnais but with a smaller standard deviation on average than that of QST indicators.

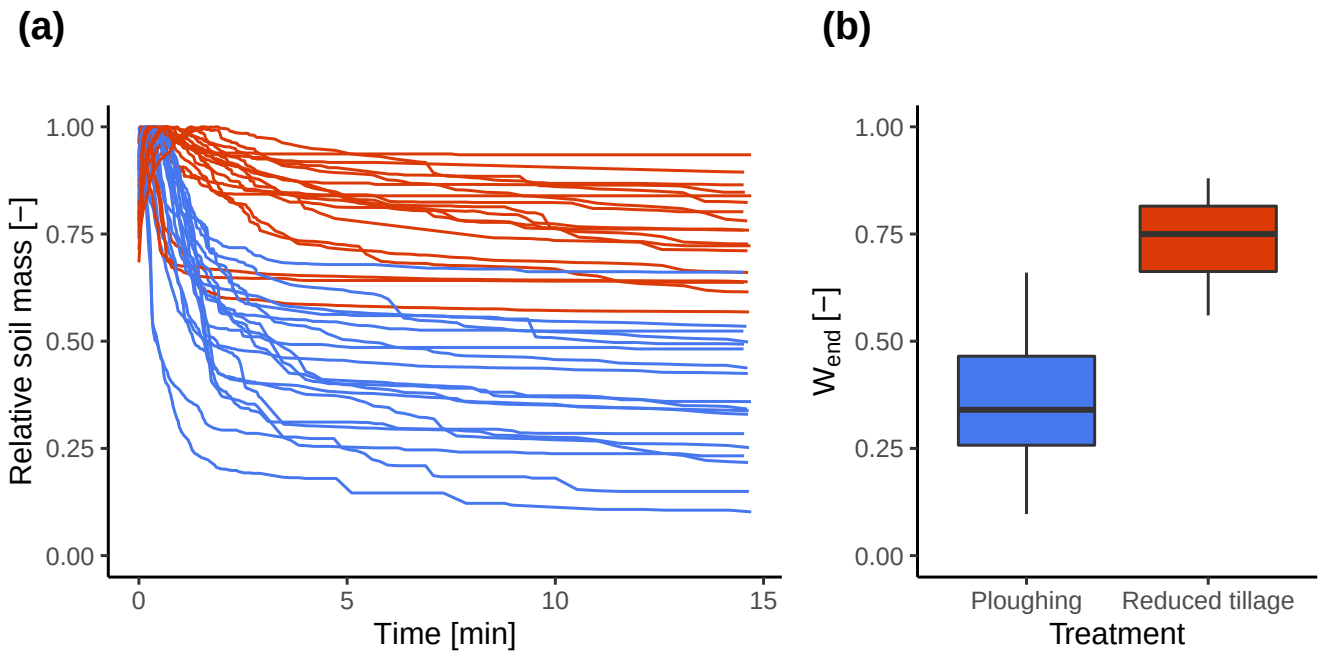

Figure 6. QST curves (a) and final relative mass (W_{end}, b) for ploughing and reduced tillage treatments of the tillage trial.

4 Discussion

4.1 Interpretation of QST curves in light of mechanisms of soil disaggregation and soil properties

4.1.1 Mechanisms of soil disaggregation

Right after immersion in water, soil mass increases due to the replacement of air by water in soil porosity. Sooner or later, soil mass then reaches a maximum before decreasing when mass loss by disaggregation exceeds mass gain due to filling of soil porosity with water. QST indicators from the start of the curves (e. g. W_{max}-W_{t0}, t_{max}, $Slope_{max-30}$) are the most correlated to the fast wetting test of Le Bissonnais (MWD1 and MA1; Table 2), which ~~indicates~~ suggests that slaking ~~significantly contributes~~ plays a major role in the initial stage of the QST. In contrast, QST indicators from the intermediate to late stages of the curves (e. g. t75 to t95) are more correlated to the slow-wetting test of Le Bissonnais (Table 2), specifically targeting clay dispersion and differential swelling. This indicates that after a longer time period under water, when soil is saturated, the effect of slaking decreases and clay dispersion and differential swelling become the dominant mechanisms of soil disaggregation. Nevertheless, both mechanisms overlap, with air release from soil further interfering with the measurement of soil mass loss when running QST. This may explain the relatively low correlation coefficients obtained between QST slopes and indicators from the fast and slow wetting tests of Le Bissonnais. It is also worth mentioning that the time of wetting of the soils of our study was relatively short (less than two minutes, as indicated by the release of air bubbles from soil). We therefore advocate that indicators from the initial

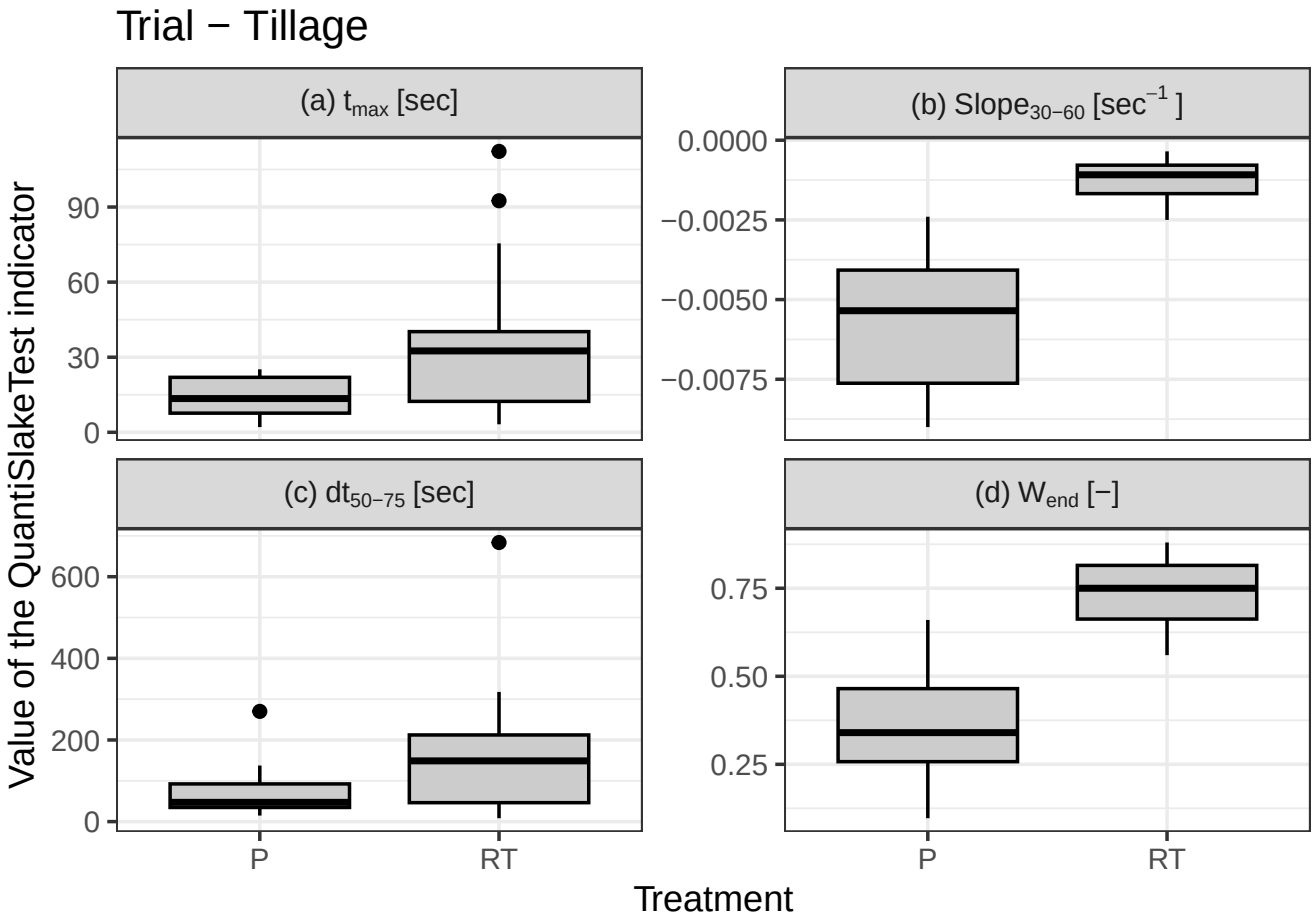

Figure 7. Boxplots of four QST indicators against tillage treatments, ploughing (P) and reduced tillage (RT) for the soils from the tillage trial. a) t_{max}; b) $Slope_{30-60}$; c) dt_{50-75}; d) W_{end}.

stage of the curve, like $Slope_{30-60}$, may provide information much more specific to slaking than indicators from the fast wetting test of Le Bissonnais, lasting ten minutes, which largely exceeds the time during which slaking is the dominant driver of disaggregation.

Except for W_{max}-W_{t0}, QST indicators correlate very poorly to the third test of Le Bissonnais, targeting soil mechanical resistance (Le Bissonnais, 1996). This indicates that little information on soil resistance to raindrop impact or shear strength from agricultural machinery can be inferred from QST curves, which is not surprising. For the soils of this study, soil mechanical resistance (as estimated by the third test of LeBissonnais) seems to be somehow controlled by the absolute clay content of soil, since clay content correlates positively to MWD3 (r=0.52) and MA3 (r=0.66).

4.1.2 The response of QST indicators to soil properties

Soil mass evolution under water as captured by QST indicators respond in an antagonist way to SOC and clay contents. Indeed, most QST indicators are positively correlated to SOC content and negatively correlated to clay content, with the absolute value of correlation coefficients decreasing for indicators of the later part of the curves ($Slope_{60\text{-}300}$, $Slope_{300\text{-}600}$ and W_{end}). Similar trends were observed in other contexts, with the resistance to slaking increasing with SOC content and decreasing with clay content (Jones et al., 2021; Francis et al., 2019). In light of the comparison between QST curves and Le Bissonnais's indicators, the amplitude of the early mass loss under water is mainly controlled by soil resistance to slaking. Accordingly, the absolute SOC content increases soil resistance to slaking, as highlighted by the positive correlation between SOC content and MWD1 (r=0.75) . The role of SOM in promoting soil aggregate stability is well-know (Chan and Mullins, 1994; Fukumasu et al., 2022; Kong et al., 2005; Regelink et al., 2015; Six et al., 2004; Tisdall and Oades, 1982), as SOM has long been recognised as one of the main binding agent in micro-aggregates (Dexter, 1988; Edwards and Bremner, 1967). The increase in SOC along a field gradient has been shown to decrease the wettability of individual aggregates ~~from~~ 3 to 5 mm in diameter and of SOM-associated clay in the $< 2\,\mu m$ fraction of soil (Chenu et al., 2000). This decrease in clay wettability might explain, in part at least, the higher aggregate stability under water of soils rich in SOC, with the slower wettability of macro-aggregates explaining their improved resistance to slaking (Chenu et al., 2000) and the slower wettability of clay decreasing its dispersive character (Chenu et al., 2000; Dexter et al., 2008).

In contrast, while the absolute clay content increases soil mechanical resistance (supported by the positive correlation with MWD3 and MA3), it also tends to decrease soil structural stability under water (as indicated by the negative correlation with most QST indicators). This supports the view that, for cropland soils of this study with low SOC content on average, clay dispersivity and differential swelling are strong drivers of soil disaggregation in wet conditions. This is in agreement with the findings of Dexter et al. (2008) who found that, for soils from France and Poland, clay has a dispersive power in water that is reduced once complexed with SOM, with an average complexation potential of 1 g of SOM for 10 g of clay. This threshold value of 0.1 for mass SOC:clay ratio was reported as pivotal between good and medium structural quality as estimated by field visual soil assessment by the CoreVESS method for 161 agricultural soils of Switzerland (Johannes et al., 2017) and for a large number of forest, grassland and cropland soils from England and Wales (Prout et al., 2020). Additionally, both Johannes et al. (2017) and Prout et al. (2020) found a linear increase in soil structural quality scores with increasing SOC:clay ratios in the range 1 : 13 to 1 : 8, suggesting that SOM has beneficial effects on soil structure beyond the threshold value of 1 : 10 determined empirically by Dexter et al. (2008). We assume that these results can be extrapolated to other temperate European soils under similar pedoclimatic conditions and clay mineralogy, as supported by the linear increase of QST indicator W_{max}-W_{t0} with the SOC:clay ratio in the range $0.04 - 0.12$ (Fig. 4). This supports the idea that W_{max}-W_{t0}, as a predictor of the SOC:clay ratio, has the potential to estimate the overall soil structural quality as measured in field conditions with visual soil assessment methods.

It is important to underline that the close linear relationship found between W_{max}-W_{t0} and the SOC:clay ratio (see Fig. 4) has probably no general character and was obtained here because cropland soils of the current study were sampled under standardised conditions of seeding and cover (winter wheat). It is very unlikely to find an identical relationship for the same

soils under contrasting conditions of soil preparation, sampling dates or crop type, since soil structure does also relate to more or less dynamic external factors such as tillage, root and hyphae development, biological activity, etc. To sum up, we suggest that the SOC:clay ratio must be seen as a proxy for soil intrinsic 'potential' structural stability, with the threshold value of 0.1 being a reasonable target for SOM management at field and farm scales (Dexter et al., 2008; Johannes et al., 2017; Prout et al., 2020). On the other hand, QST indicators such as W_{max}-W_{t0} provide a quantitative, direct measurement of the overall structural stability of a soil under a given set of conditions. Both parameters are therefore relevant in terms of appreciation of soil resistance to water erosion and structural damage by farm machinery.

4.2 The response of QST indicators to agricultural practices

One challenge for the interpretation of QST curves is the choice of the most suitable indicator(s) to assess soil structural stability. For the tillage and P-K mineral fertiliser trials, the choice of one indicator rather than another is not critical because indicators from QST curves are consistent with each other and with indicators from Le Bissonnais. In contrast, for the treatments of the organic matter trial, results differ between indicators from the start and the end of the QST curves. This originates from curves having different shapes according to the treatments, suggesting differences in disaggregation mechanisms from one treatment to another. The FYM treatment resists disaggregation more strongly at the start of the QST, whereas RR is the best treatment against disaggregation under water at the end of QST curves (Fig. 5). This last result is counter-intuitive, since the FYM treatment has a higher total SOC content than the RR treatment. Nevertheless, similar results had already been reported on the same trial (Droeven et al., 1980), with the RR treatment resisting better than FYM to disaggregation by wet sieving. This result in conflict with total SOC content must be regarded in light of (i) the quality of SOM inputs and (ii) the frequency of SOM restitution. Buysse et al. (2013a) calculated that the FYM and RR treatments receive on average similar amounts of C inputs, 472 ± 82 and $487 \pm 93\,\mathrm{gC\,m^{-2}\,y^{-1}}$, respectively. Over time, this amount of C input by farmyard manure application has led to an increase of total SOC content (about $12\,\mathrm{g\,kg^{-1}}$ for the FYM treatment) whereas for the RR treatment, an equivalent C input by green manure and residue restitution only allowed to maintain SOC content to the initial level (about $10\,\mathrm{g\,kg^{-1}}$; Buysse et al., 2013b). A smaller SOC storage for a similar C input means a higher rate of mineralisation. The formation of water-stable aggregates under the effect of microbial decomposition of root biomass is a known process (e.g, Dufey et al., 1986). In the present study, the more microbially active, labile biomass from green manure and crop residues seems to have had a stronger impact on the later part of the QST curve, controlled by clay dispersion and differential swelling, whereas the composted, stable biomass of the farmyard manure had more impact on soil resistance to slaking. This is in agreement with an important contribution of root and fungal exudates as well as microbial mucilages, known as critical binding agents in micro-aggregates (Dexter, 1988), on the reduction of clay dispersivity. Dispersive clay has been proved an important driver of soil erodibility (Brubaker et al., 1992; Czyż and Dexter, 2015). In contrast, soil resistance to slaking appears to be more related to the total content of SOC, with slaking having little effect on micro-aggregates $< 250\,\mu\mathrm{m}$ (Dexter, 1988). Another important point is the frequency of SOM inputs, with the FYM treatment receiving cattle manure once every three years whereas the RR treatment receives an extra SOM input annually, in the form of green manure or chopped straw. The last FYM application occurred almost two years before the sampling campaign.

For the tillage trial, reduced tillage (RT) improves soil structural stability regardless of the QST indicator (Fig. 7). However, indicators from the late part of QST curves ($Slope_{60\text{-}300}$, $Slope_{300\text{-}600}$) and global indicators (W_{end} and AUC) tend to discriminate better between tillage treatments. This result is consistent with an increase in both total SOC content and root biomass in the $2-7\,\mathrm{cm}$ topsoil. The gradient of concentration of SOC and nutrients from the surface soil under RT is a known effect once vertical dilution by ploughing is stopped (Chervet et al., 2016; D'Haene et al., 2009; Luo et al., 2010). This higher nutrient content in the topsoil may explain the higher root density. Whereas a higher root density is known to play a key role in soil macroaggregation, higher root density and SOC contents in the topsoil also advocate for a higher biological activity. This is in line with a better microaggregation and a better performance of indicators from the end of QST curves under RT, related to a better resistance to clay dispersion. Overall, results from the OM and the tillage long-term experiment support the view that living and labile biomass plays an important role in decreasing clay dispersion.

For the P-K mineral fertiliser trial, the ~~working~~ initial assumption that KCl application might decrease soil aggregate stability (Paradelo et al., 2016) was not verified. This might be due to a relatively short-lived disaggregating effect of KCl, since the last application occurred in the summer of 2016, almost three years before soil sampling. The beneficial effect of K fertilisation on crop production and restitution of organic matter to soil might also have counteracted a potentially negative short-term effect.

4.3 Advantages, limitations and perspectives of development of the QST test

The main strength of the QST relies on its simplicity, as the test is rapid to run and doesn't require expensive equipment or laboratory consumables: demineralised water is actually the only consumable required. QST measurements can therefore easily be repeated several times for one single plot, to improve the robustness of the result by decreasing both the impact of field microsite heterogeneity and of analytical error. Another point of attention is that the QST works on a large structured soil volume (Kopecky cylinders of $100\,\mathrm{cm}^3$ in the present study) whereas most traditional methods apply to a certain amount of small aggregates from a soil previously gently crumbled by hands (Le Bissonnais, 1996; Edwards and Bremner, 1967; Hénin et al., 1958; Kemper and Rosenau, 1986; Yoder, 1936). On the one hand, the use of a large soil volume may increase the representativeness of the soil sample while decreasing the risk of bias introduced by the selection of soil aggregates from a given size fraction: the test then neglects the properties of the soil fraction of inferior or superior equivalent diameter. On the other hand, the test is poorly adapted for a soil that has been crambled by tillage shortly before sampling, for which sampling of a soil volume of $100\,\mathrm{cm}^3$ may be complicated. Currently, the test has not been tested for stone-rich soils, for which the adequacy of the QST needs to be verified. At this point, the relevance of QST curves to assess soil erodibility needs also to be verified.

To promote the adoption of the QST method by a wide public, an open-source R-package 'slaker' (Vanwindekens and Roisin, 2022) including a web application is currently under development for QST data logging, management and analysis, including the calculation of relevant indicators and statistics from the curves and the provision of some keys of data interpretation. Therefore, the QST has a strong potential for adoption by a widespread community of end-users from soil science laboratories to farmer organisations with no or little expertise in the measurement of soil properties.

Beyond its simplicity and its large adoption potential, the dynamic character of the test is another strong point, since a high density of information ~~stands in one~~ is derived from a single curve. It offers the possibility to extract information either related to one specific mechanism of disaggregation (e.g. $Slope_{30\text{-}60}$ for slaking and t_{95} for clay dispersion) or on the overall structural stability of soil (W_{max}-W_{t0}, W_{end} or AUC). In this regard, the strong linear relationship between W_{max}-W_{t0} and SOC:clay ratio (which can be considered as a proxy for the estimation of the 'potential' structural stability of a soil, Johannes et al., 2017, Prout et al., 2020), supports the view that W_{max}-W_{t0} is relevant to evaluate the overall soil resistance to disaggregation ~~in~~ under field conditions. At the moment, curve analysis was limited to the calculation of indicators but curve modelling is another perspective of curve interpretation.

In its current state, the test doesn't provide information on the size of aggregates surviving disaggregation under water, which is of interest to predict soil susceptibility to water erosion. Nevertheless, measurement of residual aggregate size distribution with a classic sieving method would decrease the convenience of the test. As it stands, the test doesn't provide any information on soil resistance to mechanical breakdown. However, soil resistance to sealing and crusting is routinely estimated by pedotransfer functions using pH in water and SOC and clay contents as input variables (Remy and Marin-Laflèche, 1974), which appears complementary with the information offered by the QST.

~~To sum up, the QuantiSlakeTest has several strengths, some limitations and many questions currently unanswered. Number of perspectives of development exist to tackle the current issues and better exploit the curves.~~

5 Conclusions

In this work, we propose a new method to evaluate soil structural stability, the QuantiSlakeTest (QST). It consists in the dynamic weighing of a structured soil sample under water and the calculation of several indicators from the curves to evaluate soil structural stability. The QST presents several advantages. First, it is rapid to run and works with structured soil samples of large size, which improves the representativeness of the sample and allows for multiple field repetitions. Second, the QST doesn't require expensive equipment or laboratory consumables. Third, a high density of information stands in one single curve, with the possibility to extract information either on specific mechanisms of soil disaggregation (slaking or clay dispersion and differential swelling), or on the overall structural stability of soil. Therefore, the test has a strong potential for adoption by a widespread community of end-users from soil science laboratories to farmer organisations with no or little expertise in the measurement of soil properties.

In the present article, the QST was applied to 35 agricultural soil samples from three long-term experiments in the silt loam region of central Belgium. For these soils, the early mass loss under water was mainly related to slaking, whereas after soil saturation with water, clay dispersion and differential swelling became the dominant processes of soil disaggregation. We found that soil resistance to disaggregation is closely related to the SOM status of soil, well-captured by the SOC:clay ratio. From our results, we confirm the validity of the SOC:clay as a proxy for the estimation of soil intrinsic 'potential' structural stability for the soils of central Belgium, as it correlated strongly with QST indicators.

Beyond the absolute amount of SOC for a given level of clay, the response of QST indicators to soil management practices highlighted that the quality and timing of SOM inputs affects both SOC storage and soil resistance to disaggregation. In the organic matter trial, for similar total SOC inputs, farmyard manure favoured the total SOC content and had the best soil resistance to slaking whereas green manure and restitution of crop residues improved soil resistance to clay dispersion and differential swelling the most. This supports the view that living and labile biomass is more efficient in decreasing clay dispersivity whereas soil resistance to slaking relates to total SOC content. This underlines that the choice of indicators for the interpretation of QST curves must be done with great caution, as indicators from the start and the end of the curve may lead to conflicting conclusions.

Appendix A: Supplementary matrices of correlation coefficients

A1 Autocorrelations between QST indicators

Table A1. Autocorrelation coefficients between QuantiSlakeTest indicators

	Slope 0-max	tmax	Wmax-Wt0	Slope max-30	Slope 30-60	Slope 60-30	Slope 300-600	Slope max-60	Slope max-300	Slope max-600	dt max-25	dt 25-50	dt 50-75	dt 75-90	t50	t75	t90	t95	Wend	AUC
Slope 0-max	1.00	-0.57	-0.36	-0.51	-0.36	0.06	0.35	-0.52	-0.42	-0.35	-0.60	-0.49	-0.38	-0.33	-0.57	-0.48	-0.47	-0.37	-0.36	-0.42
tmax	-0.57	1.00	0.88	0.78	0.64	0.04	-0.46	0.84	0.74	0.65	0.91	0.82	0.71	0.52	0.91	0.84	0.78	0.71	0.64	0.75
Wmax-Wt0	-0.36	0.88	1.00	0.71	0.48	0.09	-0.27	0.72	0.66	0.61	0.72	0.54	0.49	0.49	0.67	0.60	0.62	0.61	0.58	0.67
Slope max-30	-0.51	0.78	0.71	1.00	0.50	-0.16	-0.42	0.94	0.71	0.65	0.82	0.66	0.52	0.40	0.78	0.67	0.62	0.54	0.62	0.74
Slope 30-60	-0.36	0.64	0.48	0.50	1.00	0.27	-0.32	0.76	0.81	0.75	0.56	0.62	0.50	0.22	0.61	0.58	0.47	0.35	0.77	0.81
Slope 60-30	0.06	0.04	0.09	-0.16	0.27	1.00	0.46	-0.02	0.51	0.60	-0.25	-0.07	-0.06	-0.08	-0.17	-0.11	-0.11	-0.15	0.61	0.48
Slope 300-600	0.35	-0.46	-0.27	-0.42	-0.32	0.46	1.00	-0.45	-0.16	0.04	-0.70	-0.50	-0.45	-0.39	-0.63	-0.56	-0.54	-0.56	0.02	-0.15
Slope max-60	-0.52	0.84	0.72	0.94	0.76	-0.02	-0.45	1.00	0.85	0.77	0.84	0.74	0.59	0.38	0.83	0.73	0.65	0.54	0.76	0.86
Slope max-300	-0.42	0.74	0.66	0.71	0.81	0.51	-0.16	0.85	1.00	0.98	0.59	0.60	0.48	0.29	0.62	0.57	0.50	0.39	0.98	1.00
Slope max-600	-0.35	0.65	0.61	0.65	0.75	0.60	0.04	0.77	0.98	1.00	0.46	0.50	0.39	0.22	0.50	0.46	0.40	0.29	0.99	0.98
dt max-25	-0.60	0.91	0.72	0.82	0.56	-0.25	-0.70	0.84	0.59	0.46	1.00	0.84	0.66	0.48	0.96	0.84	0.76	0.69	0.46	0.61
dt 25-50	-0.49	0.82	0.54	0.66	0.62	-0.07	-0.50	0.74	0.60	0.50	0.84	1.00	0.85	0.55	0.95	0.94	0.86	0.76	0.49	0.60
dt 50-75	-0.38	0.71	0.49	0.52	0.50	-0.06	-0.45	0.59	0.48	0.39	0.66	0.85	1.00	0.57	0.78	0.96	0.89	0.87	0.34	0.47
dt 75-90	-0.33	0.52	0.49	0.40	0.22	-0.08	-0.39	0.38	0.29	0.22	0.48	0.55	0.57	1.00	0.53	0.59	0.86	0.83	0.17	0.28
t50	-0.57	0.91	0.67	0.78	0.61	-0.17	-0.63	0.83	0.62	0.50	0.96	0.95	0.78	0.53	1.00	0.92	0.84	0.76	0.49	0.63
t75	-0.48	0.84	0.60	0.67	0.58	-0.11	-0.56	0.73	0.57	0.46	0.84	0.94	0.96	0.59	0.92	1.00	0.92	0.87	0.43	0.57
t90	-0.47	0.78	0.62	0.62	0.47	-0.11	-0.54	0.65	0.50	0.40	0.76	0.86	0.89	0.86	0.84	0.92	1.00	0.95	0.35	0.50
t95	-0.37	0.71	0.61	0.54	0.35	-0.15	-0.56	0.54	0.39	0.29	0.69	0.76	0.87	0.83	0.76	0.87	0.95	1.00	0.23	0.38
Wend	-0.36	0.64	0.58	0.62	0.77	0.61	0.02	0.76	0.98	0.99	0.46	0.49	0.34	0.17	0.49	0.43	0.35	0.23	1.00	0.98
AUC	-0.42	0.75	0.67	0.74	0.81	0.48	-0.15	0.86	1.00	0.98	0.61	0.60	0.47	0.28	0.63	0.57	0.50	0.38	0.98	1.00

Table A2. Correlation coefficients between soil properties, Mean Weight Diameters (MWD) and percentages of macro-aggregates (MA) from the three tests of Le Bissonnais (1. Fast wetting; 2. Slow wetting; 3. Mechanical breakdown in water after rewetting with EtOH) and soil properties. The gradient of colours relates to the positive (blue) or to the negative (orange) relative amplitude of correlation coefficients.

	SOC	Clay	SOC:Clay	pH	Bulk density
MWD 1	0.75	-0.35	0.67	-0.06	-0.29
MWD 2	0.70	-0.12	0.48	0.16	-0.30
MWD 3	0.11	0.52	-0.33	-0.31	0.31
MA 1	0.63	-0.43	0.64	-0.25	-0.20
MA 2	0.43	0.19	0.05	-0.08	0.09
MA 3	-0.07	0.66	-0.55	-0.39	0.44

A2 Soil properties and indicators from Le Bissonnais approach

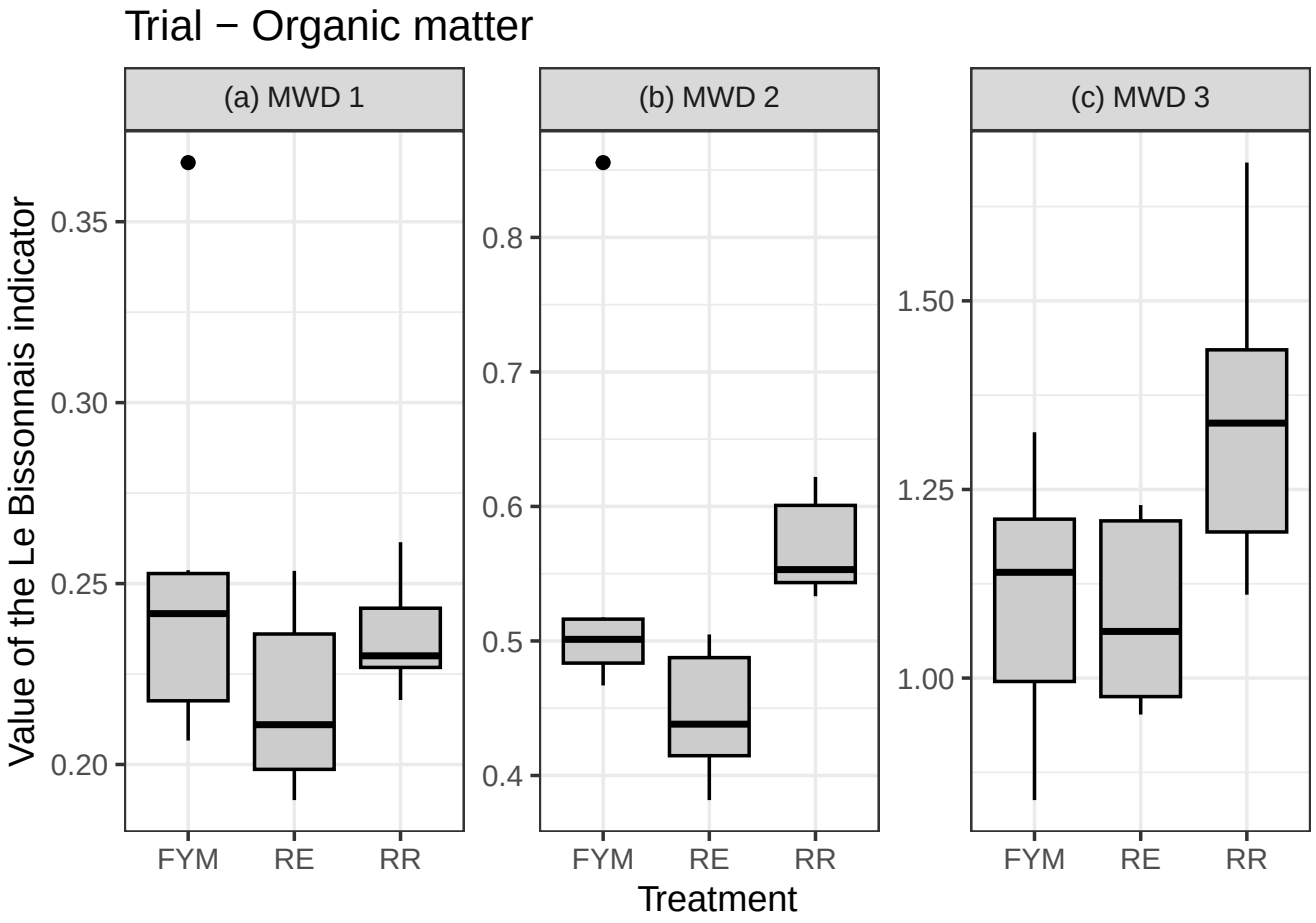

Figure B1. Boxplots of the three MWD from Le Bissonnais test against treatments of OM input for the soils from the organic matter trial, 'residue exportation' (RE), 'farmyard manure' (FYM) and 'residue restitution' (RR).

Appendix B: Le Bissonnais soil aggregate stability under contrasting soil management practices

B1 Organic matter trial

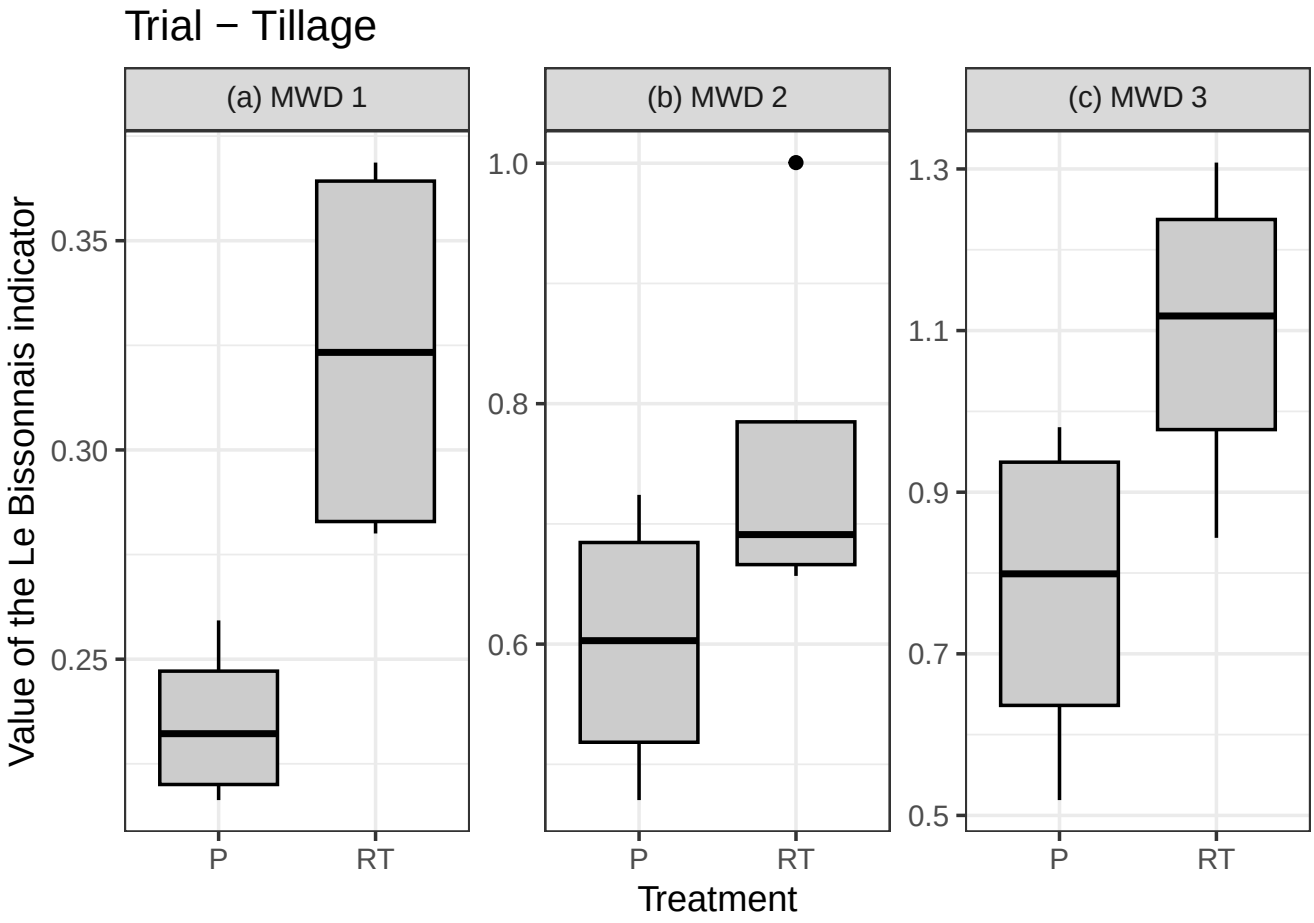

Figure B2. Boxplots of the three MWD from Le Bissonnais test against tillage treatments, ploughing (P) and reduced tillage (RT) for the soils from the tillage trial.

B2 Tillage trial

Code availability. R-package - slaker - Analysing the data of QuantiSlakeTest approach. R-package and Web Application, https://gitlab.com/FrdVnW/slaker ; Notebook with codes, figures and tables - qst-openscience, https://frdvnw.gitlab.io/qst-openscience/

Data availability. Data repository in the SlakingLab community on Zenodo https://doi.org/10.5281/zenodo.7142458

Code and data availability. Full git repository - qst-openscience https://gitlab.com/FrdVnW/qst-openscience

Video supplement. A visualisation of the QuantiSlakeTest, comparing two contrasted samples (tillage / conservation tillage) and curve generation ; Tuto slake 1, in french ; Tuto slake 2, in french

Author contributions. FV and BH planned the sampling campaign and the measurements, analysed the data, wrote the manuscript draft and reviewed and edited the manuscript.

Competing interests. The authors declare no competing interests.

Acknowledgements. Many thanks to Dr Ir Christian Roisin, whose questions and ideas initiated the development of our approach. We are grateful to the students who contributed to the development of the method by running QuantiSlakeTest for their training or thesis: Vincent Gaucet, Cyril André, Mathieu Dufey, Clément Masson, Fanny Lizin. We thank peers for useful feedbacks on the method and early results presented in international conferences. We would like to thank the two anonymous reviewers whose questions, comments and suggestions helped improve and clarify this manuscript.This study is part of the PIRAT project (CRA-W) and supported by the action plan BIO2030 (CRA-W / Wallonie).

References

Alewell, C., Borrelli, P., Meusburger, K., and Panagos, P.: Using the USLE: Chances, challenges and limitations of soil erosion modelling, International Soil and Water Conservation Research, 7, 203–225, https://doi.org/10.1016/j.iswcr.2019.05.004, 2019.

Antoine, P., Catt, J., Lautridou, J.-P., and Sommé, J.: The loess and coversands of northern France and southern England, Journal of Quaternary Science, 18, 309–318, https://doi.org/https://doi.org/10.1002/jqs, 2003.

Association Française de Normalisation: Qualité du sol - Détermination de la distribution granulométrique des particules du sol - Méthode à la pipette, Standard NF-X31-107, Association Française de Normalisation, 2003.

Association Française de Normalisation: Sludge, treated biowaste, soil and waste - Determination of total organic carbon (TOC) by dry combustion, Standard NF-EN-15936, Association Française de Normalisation, 2012.

Bagnall, D. K. and Morgan, C. L.: SLAKES and 3D Scans characterize management effects on soil structure in farm fields, Soil and Tillage Research, 208, 104 893, https://doi.org/10.1016/j.still.2020.104893, 2021.

Barthès, B. and Roose, E.: Aggregate stability as an indicator of soil susceptibility to runoff and erosion; validation at several levels, Catena, 47, 133–149, https://doi.org/10.1016/S0341-8162(01)00180-1, 2002.

Bates, D., Mächler, M., Bolker, B., and Walker, S.: Fitting Linear Mixed-Effects Models Using lme4, Journal of Statistical Software, 67, 1–48, https://doi.org/10.18637/jss.v067.i01, 2015.

Bielders, C. L., Ramelot, C., and Persoons, E.: Farmer perception of runoff and erosion and extent of flooding in the silt-loam belt of the Belgian Walloon Region, Environmental Science and Policy, 6, 85–93, https://doi.org/10.1016/S1462-9011(02)00117-X, 2003.

Brubaker, B., Holzhey, C., and Brasher, B.: Estimating the water-dispersible clay content in soils, Soil Science Society of America Journal, 56, 1226–1232, 1992.

Buysse, P., Roisin, C., and Aubinet, M.: Fifty years of contrasted residue management of an agricultural crop: Impacts on the soil carbon budget and on soil heterotrophic respiration, Agriculture, Ecosystems and Environment, 167, 52–59, https://doi.org/10.1016/j.agee.2013.01.006, 2013a.

Buysse, P., Schnepf-Kiss, A. C., Carnol, M., Malchair, S., Roisin, C., and Aubinet, M.: Fifty years of crop residue management have a limited impact on soil heterotrophic respiration, Agricultural and Forest Meteorology, 180, 102–111, https://doi.org/10.1016/j.agrformet.2013.05.004, 2013b.

Chabert, A. and Sarthou, J. P.: Conservation agriculture as a promising trade-off between conventional and organic agriculture in bundling ecosystem services, Agriculture, Ecosystems and Environment, 292, 106 815, https://doi.org/10.1016/j.agee.2019.106815, 2020.

Chan, K. Y. and Mullins, C. E.: Slaking characteristics of some Australian and British soils, European Journal of Soil Science, 45, 273–283, https://doi.org/10.1111/j.1365-2389.1994.tb00510.x, 1994.

Chenu, C., Le Bissonnais, Y., and Arrouays, D.: Organic Matter Influence on Clay Wettability and Soil Aggregate Stability, Soil Science Society of America Journal, 64, 1479–1486, https://doi.org/10.2136/sssaj2000.6441479x, 2000.

Chervet, A., Ramseier, L., Sturny, W. G., Zuber, M., Stettler, M., Weisskopf, P., Zihlmann, U., Martínez, I., and Keller, T.: Rendements et paramètres du sol après 20 ans de semis direct et de labour, Recherche agronomique suisse, 7, 216–223, 2016.

Czyż, E. A. and Dexter, A. R.: Mechanical dispersion of clay from soil into water: Readily-dispersed and spontaneously-dispersed clay, International Agrophysics, 29, 31–37, https://doi.org/10.1515/intag-2015-0007, 2015.

Dexter, A. R.: Advances in Characterization of Soil Structure, Soil and Tillage Research, 11, 199–238, 1988.

Dexter, A. R., Richard, G., Arrouays, D., Czyz, E. A., Jolivet, C., and Duval, O.: Complexed organic matter controls soil physical properties, Geoderma, 144, 620–627, https://doi.org/10.1016/j.geoderma.2008.01.022, 2008.

D'Haene, K., Sleutel, S., De Neve, S., Gabriels, D., and Hofman, G.: The effect of reduced tillage agriculture on carbon dynamics in silt loam soils, Nutrient Cycling in Agroecosystems, 84, 249–265, https://doi.org/10.1007/s10705-008-9240-9, 2009.

Droeven, G., Rixhon, L., Crohain, A., and Raimond, Y.: Evolution à long terme de la teneur en humus, de la stabilite structurale et du rendement des cultures sous l'influence de differents modes de restitution de matières organiques sur sols limoneux. Rapport interne., Tech. rep., Centre wallon de Recherches Agronomique, Gembloux, Belgium, 1980.

Dufey, J. E., Halen, H., and Frankart, R.: Evolution de la stabilité structurale du sol sous l'influence des racines de trèfle (Trifolium pratense L.) et de ray-grass (Lolium multiflorum Lmk.). Observations pendant et après culture, Agronomie, 6, 811–817, https://doi.org/10.1051/agro:19860905, 1986.

Edwards, A. and Bremner, J.: Microaggregates in soils., Journal of Soil Science, 18, 64–73., 1967.

Fajardo, M., McBratney, A. B., Field, D. J., and Minasny, B.: Soil slaking assessment using image recognition, Soil and Tillage Research, 163, 119–129, https://doi.org/10.1016/j.still.2016.05.018, 2016.

Fox, J. and Weisberg, S.: An R Companion to Applied Regression, Sage, Thousand Oaks CA, third edn., https://socialsciences.mcmaster.ca/jfox/Books/Companion/, 2019.

Francis, R., Wuddivira, M. N., Darsan, J., and Wilson, M.: Soil slaking sensitivity as influenced by soil properties in alluvial and residual humid tropical soils, Journal of Soils and Sediments, 19, 1937–1947, 2019.

Fukumasu, J., Jarvis, N., Koestel, J., Kätterer, T., and Larsbo, M.: Relations between soil organic carbon content and the pore size distribution for an arable topsoil with large variations in soil properties, European Journal of Soil Science, 73, e13 212, https://doi.org/10.1111/ejss.13212, 2022.

Goidts, E. and van Wesemael, B.: Regional assessment of soil organic carbon changes under agriculture in Southern Belgium (1955-2005), Geoderma, 141, 341–354, https://doi.org/10.1016/j.geoderma.2007.06.013, 2007.

Hadas, A.: Long-term tillage practice effects on soil aggregation modes and strength, Soil Science Society of America Journal, 51, 191–197, 1987.

Haynes, R.: Effect of sample pretreatment on aggregate stability measured by wet sieving or turbidimetry on soils of different cropping history., Journal of Soil Science, 44, 261–270, https://doi.org/http://dx.doi.org/10.1111/j.1365-2389.1993.tb00450.x, 1993.

Hénin, S., Monnier, G., and Combeau, A.: Method for the analysis of the structural stability of soils, Annales Agronomiques, 9, 71–90, 1958.

Holland, J. M.: The environmental consequences of adopting conservation tillage in Europe: Reviewing the evidence, Agriculture, Ecosystems and Environment, 103, 1–25, https://doi.org/10.1016/j.agee.2003.12.018, 2004.

Imeson, A. and Vis, M.: Assessing soil aggregate stability by waterdrop impact and utrasonic dispersion, Geoderma, 34, 185–200, https://doi.org/10.1016/0016-7061(84)90038-7, 1984.

International Organization for Standardization: Soil Quality—Determination of Organic and Total Carbon after Dry Combustion (Elementary Analysis), Standard NF-ISO-10694, International Organization for Standardization, 1995.

International Organization for Standardization: Soil quality - determination of pH, Standard ISO-10390, International Organization for Standardization, 2005.

International Organization for Standardization: Soil quality - Measurement of the stability of soil aggregates subjected to the action of water, Standard ISO/FDIS10930:2011, International Organization for Standardization, 2012.

IPCC: Climate Change 2014 Part A: Global and Sectoral Aspects, IPCC, papers2://publication/uuid/B8BF5043-C873-4AFD-97F9-A630782E590D, 2014.

IUSS Working Group WRB: World reference base for soil resources 2014. International soil classification system for naming soils and creating legends for soil maps. World Soil Resources Reports N° 106., Tech. rep., FAO, Rome, Italy, 2014.

Johannes, A., Matter, A., Schulin, R., Weisskopf, P., Baveye, P. C., and Boivin, P.: Optimal organic carbon values for soil structure quality of arable soils. Does clay content matter?, Geoderma, 302, 14–21, https://doi.org/10.1016/j.geoderma.2017.04.021, 2017.

Jones, E. J., Filippi, P., Wittig, R., Fajardo, M., Pino, V., and Mcbratney, A. B.: Mapping soil slaking index and assessing the impact of management in a mixed agricultural landscape, Soil, 7, 33–46, https://doi.org/10.5194/soil-7-33-2021, 2021.

Kemper, W. D. and Rosenau, R. C.: Aggregate stability and size distribution, in: Methods of soil analysis, part 1. Agronomy monographs no. 9, edited by Klute, A.S.A. Madison, 1986.

Koestel, J., Fukumasu, J., Garland, G., Larsbo, M., and Nimblad Svensson, D.: Approaches to delineate aggregates in intact soil using X-ray imaging, Geoderma, 402, 115 360, https://doi.org/10.1016/j.geoderma.2021.115360, 2021.

Kong, A. Y. Y., Six, J., Bryant, D. C., Denison, R. F., and van Kessel, C.: The Relationship between Carbon Input, Aggregation, and Soil Organic Carbon Stabilization in Sustainable Cropping Systems, Soil Science Society of America Journal, 69, 1078–1085, https://doi.org/10.2136/sssaj2004.0215, 2005.

Langohr, R.: L'anthropisation du paysage pédologique agricole de la Belgique depuis le Néolithique ancien: apports de l'archéopédologie, Etude Et Gestion Des Sols, 8, 103–118, 2001.

Le Bissonnais, Y.: Aggregate stability and assessment of soil crustability and erodibility: Theory and methodology, European Journal of Soil Science, 46, 425–437, 1996.

Le Bissonnais, Y. and Le Souder, C.: Measurement of aggregate stability for the assessment of soil crustability and erodibility, Étude et Gestion des Sols, 2, 43–56, 1995.

Lenth, R. V.: emmeans: Estimated Marginal Means, aka Least-Squares Means, https://CRAN.R-project.org/package=emmeans, r package version 1.7.5, 2022.

Levy, G. J. and Mamedov, A. I.: High-Energy-Moisture-Characteristic Aggregate Stability as a Predictor for Seal Formation, Soil Science Society of America Journal, 66, 1603–1609, https://doi.org/10.2136/sssaj2002.1603, 2002.

Loch, R. J.: Aggregate breakdown under rain : its measurement and interpretation, Ph.D. thesis, University of New England, Australia., 1989.

Luo, L., Lin, H., and Schmidt, J.: Quantitative Relationships between Soil Macropore Characteristics and Preferential Fow and Transport, Soil Science Society of America Journal, 74, 1929–1937, 2010.

Maugnard, A., Bielders, C., Bock, L., Colinet, G., Cordonnier, H., Degré, A., Demarcin, P., Dewez, A., Feltz, N., Legrain, X., Pineux, N., and Mokadem, A. I.: Cartographie du risque d'érosion hydrique à l'échelle parcellaire en soutien à la politique agricole wallonne (Belgique), Etudes et Gestion des Sols, 20, 127–141, 2013.

Mbagwu, J. S. and Auerswald, K.: Relationship of percolation stability of soil aggregates to land use, selected properties, structural indices and simulated rainfall erosion, Soil and Tillage Research, 50, 197–206, https://doi.org/10.1016/S0167-1987(99)00006-9, 1999.

Meersmans, J., Van Wesemael, B., De Ridder, F., Dotti, M. F., De Baets, S., and Van Molle, M.: Changes in organic carbon distribution with depth in agricultural soils in northern Belgium, 1960-2006, Global Change Biology, 15, 2739–2750, https://doi.org/10.1111/j.1365-2486.2009.01855.x, 2009.

Meersmans, J., Van Wesemael, B., Goidts, E., Van Molle, M., De Baets, S., and De Ridder, F.: Spatial analysis of soil organic carbon evolution in Belgian croplands and grasslands, 1960-2006, Global Change Biology, 17, 466–479, https://doi.org/10.1111/j.1365-2486.2010.02183.x, 2011.

Paradelo, R., van Oort, F., Barré, P., Billiou, D., and Chenu, C.: Soil organic matter stabilization at the pluri-decadal scale: Insight from bare fallow soils with contrasting physicochemical properties and macrostructures, Geoderma, 275, 48–54, https://doi.org/https://doi.org/10.1016/j.geoderma.2016.04.009, 2016.

Prout, J. M., Shepherd, K. D., McGrath, S. P., Kirk, G. J., and Haefele, S. M.: What is a good level of soil organic matter? An index based on organic carbon to clay ratio, European Journal of Soil Science, pp. 1–11, https://doi.org/10.1111/ejss.13012, 2020.

R Core Team: R: A Language and Environment for Statistical Computing, R Foundation for Statistical Computing, Vienna, Austria, https://www.R-project.org/, 2023.

Regelink, I. C., Stoof, C. R., Rousseva, S., Weng, L., Lair, G. J., Kram, P., Nikolaidis, N. P., Kercheva, M., Banwart, S., and Comans, R. N.: Linkages between aggregate formation, porosity and soil chemical properties, Geoderma, 247-248, 24–37, https://doi.org/10.1016/j.geoderma.2015.01.022, 2015.

Remy, J.-C. and Marin-Laflèche, A.: L'analyse de terre : réalisation d'un programme d'interprétation automatique, Annales Agronomiques, 25, 607–632, 1974.

Roisin, C.: Essai permanent sur la gestion de la matière organique. Etat des lieux, résultats et réflexions., Tech. rep., Centre wallon de Recherches Agronomiques, Gembloux, Belgium, 2018.

Roisin, C.: Essai Longue durée sur la gestion de la fumure P-K. Etat des lieux, résultats et réflexions, Tech. rep., Centre wallon de Recherches Agronomiques, Gembloux, Belgium, 2019.

Seitz, S., Goebes, P., Puerta, V. L., Pereira, E. I. P., Wittwer, R., Six, J., van der Heijden, M. G., and Scholten, T.: Conservation tillage and organic farming reduce soil erosion, https://doi.org/10.1007/s13593-018-0545-z, 2019.

Shi, P., Castaldi, F., van Wesemael, B., and Van Oost, K.: Vis-NIR spectroscopic assessment of soil aggregate stability and aggregate size distribution in the Belgian Loam Belt, Geoderma, 357, 113 958, https://doi.org/10.1016/j.geoderma.2019.113958, 2020.

Six, J., Bossuyt, H., Degryze, S., and Denef, K.: A history of research on the link between (micro)aggregates, soil biota, and soil organic matter dynamics, Soil and Tillage Research, 79, 7–31, https://doi.org/10.1016/j.still.2004.03.008, 2004.

Tisdall, J. M. and Oades, J. M.: Organic matter and water-stable aggregates in soils, Journal of Soil Science, 33, 141–163., 1982.

Vancampenhout, K., Langohr, R., Slaets, J., Buurman, P., Swennen, R., and Deckers, J.: Paleo-pedological record of the Rocourt Pedosequence at Veldwezelt–Hezerwater (Belgian Pleistocene loess belt): Part 1—Evolution of the parent material, Catena, 107, 118–129, 2013.

Vanwindekens, F. and Roisin, C.: slaker: Conduct and visualize QuantiSlakeTest of soil samples, https://gitlab.com/FrdVnW/slaker, r package version 0.2, 2022.

Wuddivira, M. N., Stone, R. J., and Ekwue, E. I.: Clay, Organic Matter, and Wetting Effects on Splash Detachment and Aggregate Breakdown under Intense Rainfall, Soil Science Society of America Journal, 73, 226–232, https://doi.org/10.2136/sssaj2008.0053, 2009.

Yoder, R. E.: A direct method of aggregate analysis of soils and a study of the physical nature of erosion losses, Journal of American Society of Agronomy, 28, 337–351, 1936.

Zhu, Y., Marchuk, A., and McLean Bennett, J.: Rapid Method for Assessment of Soil Structural Stability by Turbidimeter, Soil Science Society of America Journal, 80, 1629–1637, https://doi.org/10.2136/sssaj2016.07.0222, 2016.